



Synthesis and biological evaluation of novel isoxazole-piperazine hybrids as potential anti-cancer agents with inhibitory effect on liver cancer stem cells



Kübra İbiş^{a,1}, Esra Nalbat^{b,1}, Burcu Çalışkan^a, Deniz Cansen Kahraman^b, Rengul Cetin-Atalay^{b,**}, Erden Banoglu^{a,*}

^a Department of Pharmaceutical Chemistry, Faculty of Pharmacy, Gazi University, Ankara, Turkey

^b Graduate School of Informatics, Cancer Systems Biology Laboratory, ODTU, Ankara, Turkey

ARTICLE INFO

Article history:

Received 8 March 2021

Received in revised form

15 April 2021

Accepted 16 April 2021

Available online 24 April 2021

Keywords:

Cancer
Liver
Isoxazole
Piperazine
Cancer stem cell

ABSTRACT

In our effort for the development of novel anticancer therapeutics, a series of isoxazole-piperazine analogues were prepared, and primarily screened for their antiproliferative potential against hepatocellular carcinoma (HCC; Huh7/Mahlavu) and breast (MCF-7) cancer cells. All compounds demonstrated potent to moderate cytotoxicity on all cell lines with IC₅₀ values in the range of 0.09–11.7 μM. Further biological studies with **6a** and **13d** in HCC cells have shown that both compounds induced G1 or G2/M arrests resulting in apoptotic cell death. Subsequent analysis of proteins involved in cell cycle progression as well as proliferation of HCC cells revealed that **6a** and **13d** may affect cellular survival pathways differently depending on the mutation profiles of cells (p53 and PTEN), epidermal/mesenchymal characteristics, and activation of cell mechanisms through p53 dependent/independent pathways. Lastly, we have demonstrated the potential anti-stemness properties of these compounds in which the proportion of liver CSCs in Huh7 cells (CD133+/EpCAM+) were significantly reduced by **6a** and **13d**. Furthermore, both compounds caused a significant reduction in expression of stemness markers, NANOG or OCT4 proteins, in Mahlavu and Huh7 cells, as well as resulted in a decreased sphere formation capacity in Huh7 cells. Together, these novel isoxazole-piperazine derivatives may possess potential as leads for development of effective anti-cancer drugs against HCC cells with stem cell-like properties.

© 2021 Elsevier Masson SAS. All rights reserved.

1. Introduction

Cancer is a multifactorial disease, which is simultaneously concerted by a combination of genetic, epigenetic, and environmental factors, and is one of the leading cause of deaths globally [1,2]. Hepatocellular carcinoma (HCC) is the most common type of liver cancer accounting for about 75% of all primary liver cancers, and is the 6th most frequent and the 2nd deadly cancer worldwide [3–5]. Due to its various promoting factors (HBV, HCV, Aflatoxins, obesity) HCC presents with high inter and intra tumor heterogeneity [6], and the development new cancer therapeutics against

these cancer types are significantly hampered, and many candidate drugs did not produce clinical benefit in the overall population [7]. In most cases, although the developed new agents initially demonstrate efficacy, drug resistance is often seen as an inevitable consequence of cancer's heterogeneity and is therefore likely to underpin failures of the drug development for HCC therapy. One of the reasons of these failures in HCC patients is the enrichment of cancer stem cells (CSC), which are able to self-renew and differentiate into cancer cells resulting in acquired resistance to drug therapy as shown in sorafenib-resistant liver cancer cells [8–10]. Therefore, an endless effort has continuously been devoted to the discovery and development of new and more effective anti-cancer agents that are capable to intervene with these complex diseases.

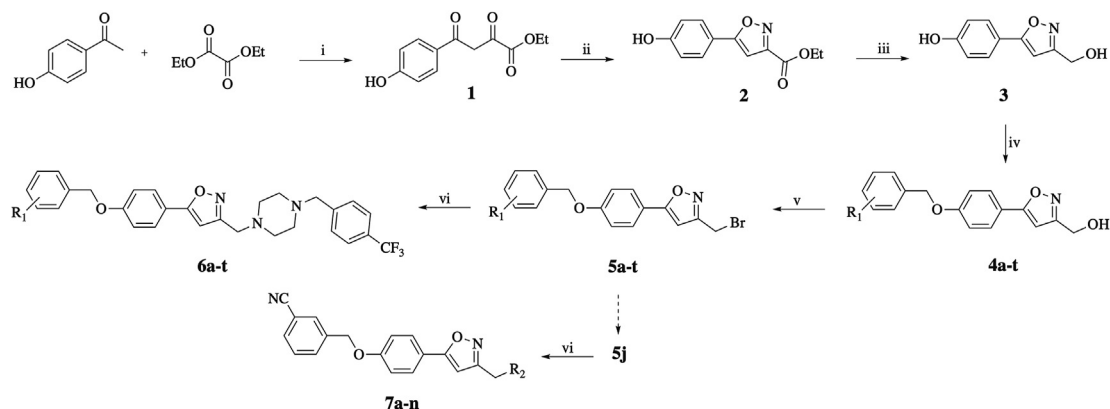
Small molecule inhibitors (SMIs) comprise the most extensively studied cancer therapeutics having the advantage to translocate through the plasma membrane and interact with the cytoplasmic domain of cell-surface receptors and intracellular signaling pathways [11,12]. Isoxazole derivatives as SMIs have been in the center

* Corresponding author.

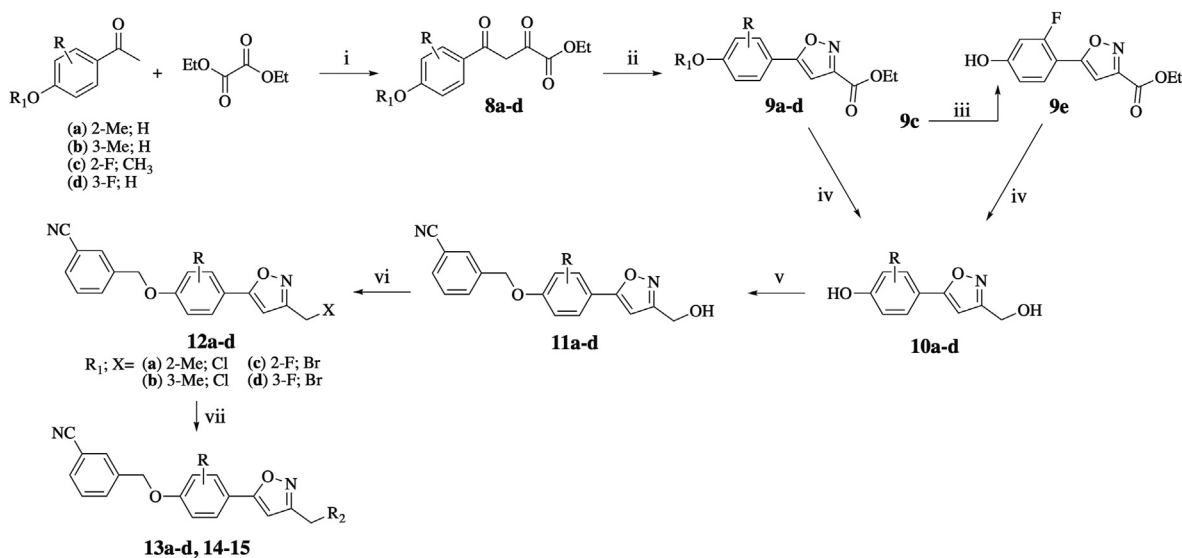
** Corresponding author.

E-mail addresses: rengul@metu.edu.tr (R. Cetin-Atalay), banoglu@gazi.edu.tr (E. Banoglu).

¹ Equal Contribution.



Scheme 1. Synthesis of Compounds **6a-t** and **7a-n**. Reagents and conditions: i) NaOEt, EtOH; ii) NH₂OH·HCl, EtOH; iii) LiAlH₄, THF; iv) BnBr derivatives, K₂CO₃, AcCN; v) CBr₄, PPh₃, CH₂Cl₂; vi) Amine derivatives, DIEA, DMF (R₁ and R₂ groups are given in Tables 1 and 2).



Scheme 2. Synthesis of Compounds **13a-d** and **14-15**. Reagents and conditions: i) NaOEt, EtOH; ii) NH₂OH·HCl, EtOH; iii) BBr₃, DCM; iv) LiAlH₄, THF; v) 3-CNbnBr, K₂CO₃, AcCN; vi) CBr₄, PPh₃, CH₂Cl₂ for **12c-d** or SOCl₂, DMF, CH₂Cl₂ for **12a-b** vii) Amine derivatives, DIEA, DMF.

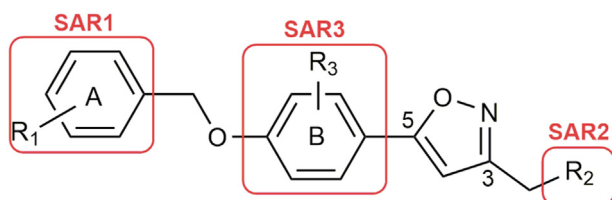


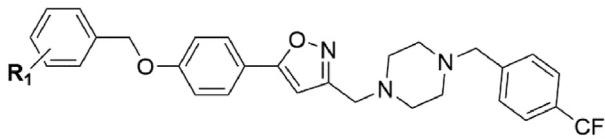
Fig. 2. Major structural modifications about the isoxazole scaffold.

against Huh7 and MCF-7 was more pronounced (IC₅₀ = 1.7 and 2.9 μM, respectively). Although no obvious structure-activity relationships (SAR) can be drawn from the cytotoxicity data of **6a-t**, it is clearly seen that certain substitutions demonstrated significant contribution to the potency and selectivity of the compounds against one or two of the cell lines tested. For example, among the chlorine substituted analogues (**6f-h**), analogue **6g** with 3-Cl-benzyl group was identified as the most highly active compound against Huh7 (IC₅₀ = 0.2 μM). Meanwhile, compounds bearing cyano (**6i-k**) and methoxy (**6o-t**) substitutions also displayed very potent antiproliferative activity for one or the two of the Huh7 and

MCF-7 cell lines. Among them, **6j** with 3-CN and **6o** with 2-OMe showed good potency and selectivity for both Huh7 (IC₅₀ = 0.1 and 0.8 μM, respectively) and MCF-7 (IC₅₀ = 0.8 and 0.3 μM, respectively), while their activity against Mahlavu cell lines were less pronounced (Table 1). In addition, both **6k** with 4-CN and **6s** with 3,5-diOMe showed clear preference for MCF-7 cell lines with IC₅₀ of 0.1 μM. Lastly, **6e** (3,5-diMe), **6p** (3-OMe) and **6t** (3,4,5-triOMe) were identified as the most highly active compounds within the series against Huh7 cancer cell line with IC₅₀ values at 0.6, 0.8, and 0.5 μM, respectively. However, none of the analogues demonstrated significant activity against Mahlavu cell lines as they did for Huh7 and MCF-7 cell lines (Table 1).

Based on the first screening, 3-CN (**6j**) was selected as the preferred substitution for further optimization, and our research was focused on the modification of piperazine ring at the right part of the scaffold. As shown in Table 2, we randomly investigated the effect of various aryl groups, i.e., differently substituted phenyl or benzyl groups, of piperazine ring of the scaffold. The results demonstrated that all compounds **7a-i**, modified by introduction of substituted benzyl or phenylpiperazines, showed moderate anti-tumor activities with IC₅₀ values in the range of 1.4–8.4 μM for MCF-7 and 1.5–6.1 μM for Huh7 as compared to the corresponding

Table 1
In vitro cytotoxic activities of **6a-t** with 72 h of treatment.



| Cmpd No | R ₁ | IC ₅₀ (μM) | | |
|-----------|----------------|-----------------------|------|---------|
| | | MCF7 | Huh7 | Mahlavu |
| 6a | H | 2.9 | 1.7 | 11.7 |
| 6b | 2-Me | 3.7 | 1.2 | 6.8 |
| 6c | 3-Me | 4.0 | 5.0 | 2.5 |
| 6d | 4-Me | 1.2 | 1.5 | 7.5 |
| 6e | 3,5-diMe | 1.6 | 0.6 | 6.0 |
| 6f | 2-Cl | 2.8 | 1.0 | 3.2 |
| 6g | 3-Cl | 1.4 | 0.2 | 4.1 |
| 6h | 4-Cl | 6.7 | 4.0 | 3.7 |
| 6i | 2-CN | 4.0 | 5.0 | 3.5 |
| 6j | 3-CN | 0.8 | 0.1 | 10.6 |
| 6k | 4-CN | 0.1 | 1.0 | 4.3 |
| 6l | 2-F | 3.0 | 1.5 | 3.1 |
| 6m | 3-F | 2.5 | 1.3 | 2.9 |
| 6n | 4-F | 7.9 | 2.0 | 3.1 |
| 6o | 2-OMe | 0.3 | 0.9 | 3.9 |
| 6p | 3-OMe | 2.0 | 0.8 | 1.4 |
| 6r | 4-OMe | 1.3 | 3.2 | 4.9 |
| 6s | 3,5-diOMe | 0.1 | 1.5 | 4.3 |
| 6t | 3,4,5-triOMe | 1.8 | 0.5 | 5.8 |

IC₅₀ values were calculated from the cell growth inhibition percentages obtained with five different concentrations in triplicates ($R^2 > 0.9$).

analogue **6j** with 4-CF₃-benzylpiperazine against MCF-7 (IC₅₀ = 0.8 μM) and Huh7 (IC₅₀ = 0.1 μM). There was a slight improvement of potency against Mahlavu cells with IC₅₀ of 1.3–5.6 μM (**6j**, IC₅₀ = 10.6 μM for Mahlavu). Although two additional aminopiperidine derivatives (**7m-n**) were also tested as opposed to piperazine ring, the activity was also moderate with IC₅₀ = 2.1–3.0 μM for all three cell lines. Unfortunately, all these derivatives led to less active than corresponding **6j** against MCF-7 and Huh7 cell lines with a moderate improvement in activity against Mahlavu cells.

Since the desired shift in structure-activity space is not achieved with this strategy, we decided to investigate the substituent effect on the middle phenyl ring (B) of the **6j** to gain further insight on the SAR at C (5) position of the isoxazole nucleus. To our delight, all of the derivatives (**13a-d**) with methyl or fluorine at 2 or 3 positions as R₃ group (Fig. 2) exhibited excellent antiproliferative activities in the single-digit micromolar range against MCF-7, Huh7, and Mahlavu cells (Table 3). Noteworthy, analogues **13b** and **13d** substituted with methyl and fluorine at 3 position, respectively, exhibited much greater antitumor activities than **6j** in MCF-7, Huh7, and Mahlavu cell lines with IC₅₀ values in the range of 0.09–0.5 μM. We also synthesized two different amine analogues (**14–15**) of the most potent **13d**, however, the potency was decreased indicating the necessity of 4-CF₃-Bn-piperazine for optimum activity. Based on these encouraging results with these isoxazole-piperazine hybrids, we selected the most potent **13d** as well as the unsubstituted **6a** for comparison for further bioactivity analysis focusing on primary liver cancer cells since there is a limited number of targeted small molecule drugs available for this cancer.

2.3. Real-time cellular response of HCC cells with compounds **6a** and **13d** treatment

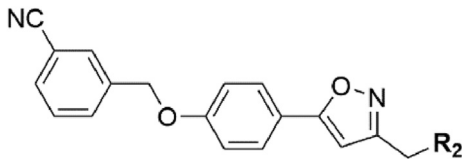
Time and dose-dependent cytotoxic activities of **6a** and **13d** were evaluated on both epithelial (Huh7 and HepG2), and

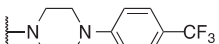
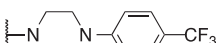
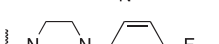
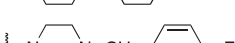
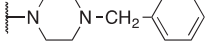
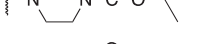
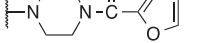
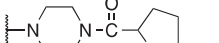
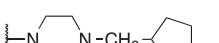
mesenchymal (Mahlavu and SNU-475) liver cancer cell lines with the use of RT-CES (xCELLigence) system. It was shown that both **6a** and **13d** displayed time and dose-dependent cell growth inhibitory effects compared to the corresponding control groups (vehicle-DMSO). The label-free dynamic monitoring results suggested that compounds generate a dose-dependent kinetic pattern characteristic, where growth inhibition begins after 40–50 h in Huh7 and SNU-475 cells, whereas this effect is seen after 90 h of treatment in Mahlavu and HepG2 cells. The cytotoxic effects of compounds reach to their highest values upon 90, 130, 150 and 90 h in Mahlavu, SNU-475, Huh7, and HepG2 cells, respectively. Many studies revealed that RT-CES system can determine cell growth inhibition and apoptosis in addition to cell growth rate and cell proliferation with changes of cell index measurements (which indicate the degree of the cell growth) from an exponentially growing state to a steady state [40]. Therefore, these dynamic changes in cell index pattern measurements might be related to the cells which undergo cell cycle arrest or cell death in our compound treated mesenchymal and epithelial liver cancer cells. In addition, the cell index values of both **6a** and **13d** treated cells with 2.5–10 μM concentrations acquired with the RT-CES results correlated with the initial findings of SRB assay results (Table S1). Data obtained from the RT-CES system showed a continuous increase in the cell growth inhibition and, hence, it is concluded that these compounds exhibit cytotoxic rather than cytostatic effects (Fig. 3).

2.4. Cell cycle arrest induced by **6a** and **13d** on HCC cells

To detect the effects of **6a** and **13d** on the cell cycle, Huh7, HepG2, SNU-475, and Mahlavu cells analyzed by flow cytometry and nuclear staining PI (Fig. 4A and Table S2). Following 48 h treatment with **6a** and **13d**, cell cycle arrest at the G0/G1 phase and an increase in the percentages of sub-G1 phase was observed in Mahlavu cells. SNU-475 cells treated with **6a** and **13d** resulted in an increase in S and G2/M phases after 48 h Huh7 cells treated with

Table 2
In vitro cytotoxic activities of **7a-n** with 72 h of treatment.



| Cmpd No | R ₂ | IC ₅₀ (μM) | | |
|-----------|---|-----------------------|------|---------|
| | | MCF7 | Huh7 | Mahlavu |
| 7a |  | 2.0 | 2.2 | 2.7 |
| 7b |  | 1.4 | 1.7 | 1.3 |
| 7c |  | 2.4 | 1.5 | 2.2 |
| 7d |  | 1.8 | 1.6 | 1.5 |
| 7e |  | 1.4 | 2.4 | 2.3 |
| 7f |  | 2.4 | 2.7 | 2.6 |
| 7g |  | 3.8 | 6.1 | 5.6 |
| 7h |  | 1.9 | 2.0 | 2.2 |
| 7i |  | 3.8 | 2.2 | 4.1 |
| 7j |  | 8.4 | 4.2 | 4.8 |
| 7k |  | 7.6 | 2.8 | 4.4 |
| 7l |  | 3.5 | 2.9 | 3.2 |
| 7m |  | 2.5 | 2.5 | 2.1 |
| 7n |  | 2.8 | 1.5 | 3.0 |

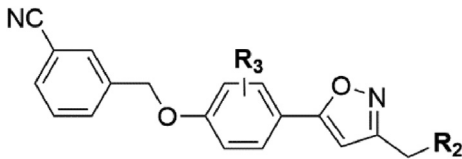
IC₅₀ values were calculated from the cell growth inhibition percentages obtained with five different concentrations in triplicates ($R^2 > 0.9$).

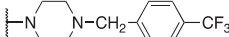
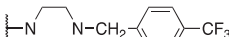
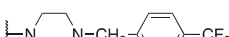
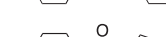
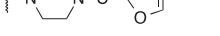
both **6a** and **13d** displayed higher cell populations in G2/M phase after 48 h. An increase in the percentages of G0/G1 phase in HepG2 cells was observed for both **6a** and **13d** at similar time points. Overall, results have shown that **6a** and **13d** induce cell cycle arrest in four HCC cell lines. When dynamic monitoring results of HCC cells are revisited, it was observed that compounds that caused G0/G1 arrest caused growth inhibition in later stages while cells that entered G2/M arrest showed earlier growth inhibition. Besides, cell cycle analysis results were correlated with the real-time growth inhibition patterns, which further supported the findings that the growth inhibition is initiated after 48 h in HCC cells.

2.5. Characterization of cell death mechanism induced by **6a** and **13d**

To observe the cell death mechanism induced by **6a** and **13d**, Annexin V staining by flow cytometry and Hoechst staining under fluorescence microscopy were performed for Mahlavu, SNU-475, Huh7 and HepG2 cells. Compared to the control group, the percentage of apoptotic populations in all cells treated with **6a** or **13d** was increased after 72 h (Fig. 4B). Both compounds caused apoptotic morphological changes (chromatin condensation, nuclear fragmentation, and apoptotic bodies) in the HCC cells after

Table 3
In vitro cytotoxic activities of **13a–d** and **14–15** with 72 h of treatment.



| Cmpd No | R ₃ | R ₂ | IC ₅₀ (μM) | | |
|------------|----------------|---|-----------------------|------|---------|
| | | | MCF7 | Huh7 | Mahlavu |
| 13a | 2-Me |  | 0.4 | 1.5 | 0.5 |
| 13b | 3-Me |  | 0.7 | 0.6 | 0.45 |
| 13c | 2-F |  | 1.2 | 0.4 | 0.4 |
| 13d | 3-F |  | 0.38 | 0.09 | 0.5 |
| 14 | 3-F |  | 1.5 | 8.1 | 3.6 |
| 15 | 3-F |  | 2.7 | 2.3 | 2.7 |

IC₅₀ values were calculated from the cell growth inhibition percentages obtained with five different concentrations in triplicates ($R^2 > 0.9$).

48 h treatment (Fig. 4C). Altogether, it was concluded that apoptotic cell death was induced in HCC cells by the selected compounds.

2.6. Analysis of cellular pathways targeted by **6a** and **13d**

Many studies revealed that p53 is a highly inducible transcription factor by various stress signals such as DNA damage, drug stress, oncogene activation, and nutrient deprivation. Mostly, the outcomes of p53 activation are cell cycle arrest and apoptosis, which are vital mechanisms for inhibiting tumor progression [41]. Some studies also showed that activation of p21/WAF1 may lead to cell cycle arrest by p53 [42,43]. In addition to regulation of cell cycle arrest, p21 also has other functions on regulation of some cellular mechanisms such as apoptosis and DNA damage response. This is related to the effects of p21 on the evolution of tumors, which depends on the level of p53 expression profiles and this leads to different levels of basal p21 protein in cancer cells [44]. Four different hepatoma-derived cell lines Mahlavu, SNU-475, Huh7, and HepG2 have different expression [45,46]. HepG2 cells have normal p53 expression [45], while SNU-475 (A239G, T275C, A288G) [46], Mahlavu (G249T), and Huh7 (C220T) [45] have mutations on p53 gene. Expression of p21 has been shown to be transcriptionally regulated by p53 [45]. On the other hand, many studies have suggested that p21 may also be regulated by p53-independent pathways [47]. Thus, we also checked whether activation of p53 protein has a role in the regulation of cell cycle and apoptosis in HCC cells upon treatment with selected compounds. While phosphorylation of p53 protein at serine 15 is elevated to induce cell cycle arrest and apoptosis [48] its acetylation at Lys382 enhances its tumor suppressive activity [49]. Our results have shown that both phospho-p53(S15) and acetyl-p53(K382) levels were increased upon treatment with **13d** in SNU-475 cells. **6a** treated SNU-475 cells showed only an increase in the phospho-p53(S15) levels. While increased levels of phospho-p53(S15) and acetyl-p53(K382) were observed in **6a** treated Mahlavu cells, **13d** treatment only induced an increase in

acetyl-p53(K382) levels. Overall, compared to **13d**, **6a** was shown to induce activity of p53 more prominently. On the other hand, both compounds did not alter p53 activity status in epithelial HCC cells (Huh7 and HepG2, data not shown). Both compounds led to increase in levels of p21 protein in SNU-475 cells, while no p21 protein expression was seen in Mahlavu cells due to p53 mutation in these cells [45] (Fig. 5A). These results might indicate that both compounds act on cell cycle regulation and apoptosis through p53 dependent mechanisms [41] in mesenchymal HCC cells.

Numerous studies have also revealed that PI3K/Akt signaling pathway has a crucial role in the progression of HCC, and is involved in various mechanisms such as cell proliferation, apoptosis, invasion, and metastasis as well as cell cycle progression [50–54]. Akt is one of the main components of PI3K/Akt signaling pathway which has major roles in both cell survival and resistance to tumor therapy [55]. Mahlavu cells and SNU-475 cells have hyperactivated Akt pathway due to the loss of PTEN protein, while the pathway is normoactive in PTEN adequate Huh7 and HepG2 cells [56,57]. Therefore, the poorly differentiated Mahlavu and SNU-475 cells represent an aggressive HCC phenotype. Upon the findings that compounds **6a** and **13d** led to cell cycle arrest and apoptosis, several targets involved in these pathways at the protein level were further investigated by Western blot analysis. Results have shown that there was a decrease in expression levels of the activated form of Akt (phospho-Akt (Ser473)) in Mahlavu cells upon treatment with the both compounds, while only **13d** decreased the phospho-Akt (S473) levels in SNU-475 cells. However, no detectable p-Akt was observed in Huh7 and HepG2 cells which is expected due to normoactive Akt pathway in these cells (data not shown). c-Myc is an oncogene, downstream of AKT, and mostly overexpressed in cancer [58]. Since it has been reported that the PI3K/AKT/mTOR pathway increases the expression of c-Myc [59], we checked the expression of c-Myc in mesenchymal HCC cells. Treatment with **6a** and **13d** in Mahlavu cells resulted in a decrease in c-Myc expression (Fig. 5B). These results revealed that our compounds have effects on

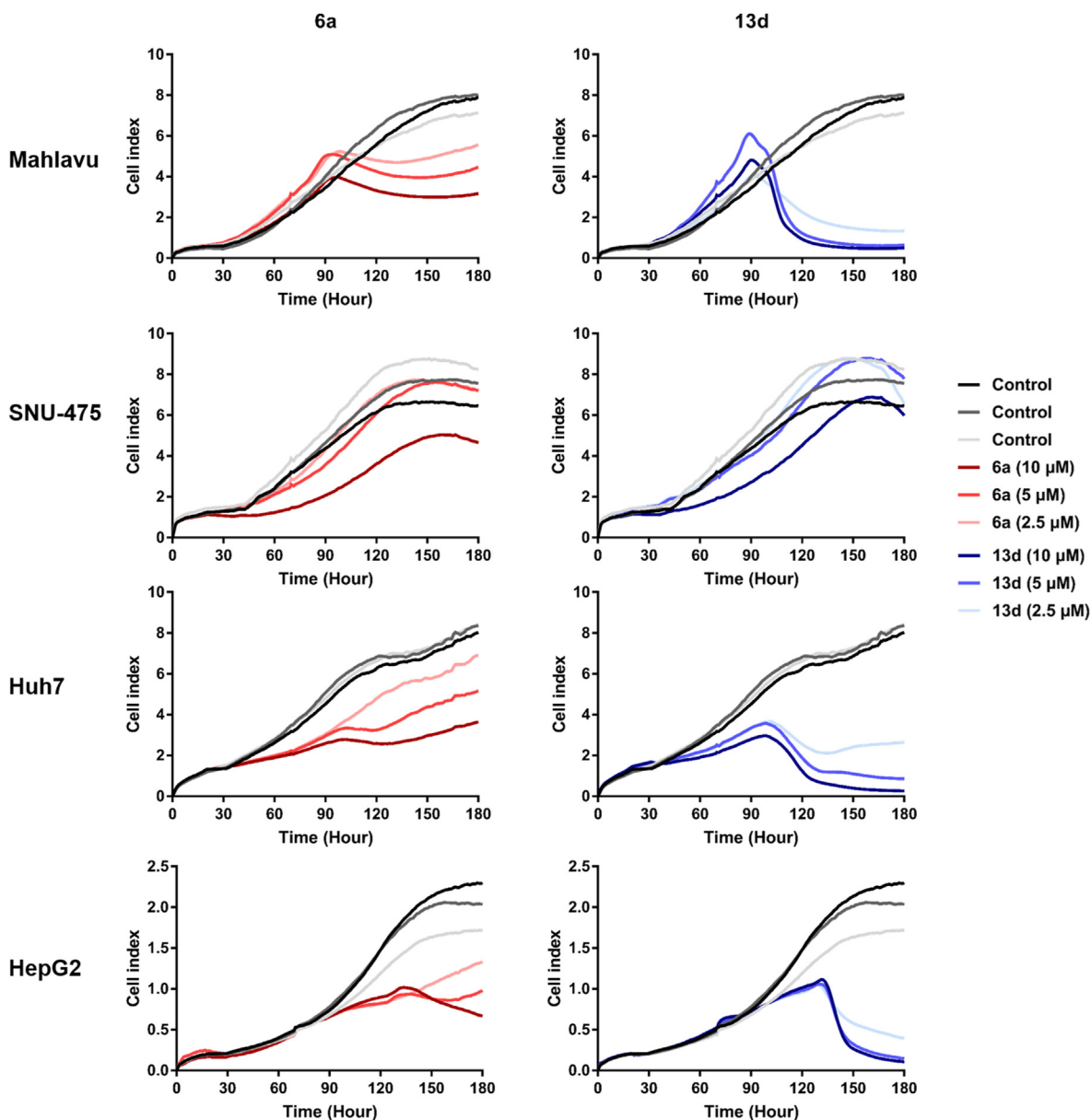


Fig. 3. Real time cellular response of Mahlavu, SNU-475, Huh7, and HepG2 hepatocellular carcinoma cells treated with compounds **6a** and **13d** and DMSO control for 180 h. The experiment was performed in triplicates and results were normalized to DMSO vehicle controls of 10–5–2.5 μM concentrations **6a** and **13d**.

PI3K/AKT/c-Myc signaling pathway. Emerging studies have suggested that PTEN may also regulate the MAPK pathway [60,61]. It is known that ERK has a role in cell migration which is vital for cancer invasion [62]. Besides, many studies revealed that cancer stem cells (CSCs) may be responsible for initiation of the tumor, the migration of cancer cells to distant tissues, and resistance to drugs [63]. A recent study revealed that there is a positive correlation between CSC markers and phospho-ERK in cancer [64]. Thus, we also analyzed the expression level of ERK1/2 protein in both **6a** and **13d** treated HCC cells. **6a** and **13d** treatment decreased the levels of active form of ERK1/2 (phospho-ERK1/2 (T202/Y204) in all HCC cells (Fig. 5C).

As a result, our data suggest that these compounds affect cellular survival pathways differently depending on the mutation profiles of cells (p53 and PTEN), epidermal/mesenchymal characteristics, and activation of cell mechanisms through p53 dependent/independent pathways in HCC cells.

2.7. **6a** and **13d** inhibits liver cancer stem cells associated traits

It is critical to identify novel compounds that can change the enrichment of the cancer stem cell (CSC) population which is responsible for the occurrence, development, relapse, drug resistance and metastasis in histopathologically heterogeneous cancers including hepatocellular carcinoma [65]. As we previously show that liver cancer stem cells (LCSCs) bear several stemness surface markers such as CD133 and EpCAM [9], which both promote sphere formation, stemness gene expression and tumorigenicity. Huh7 cells contain CD133 and EpCAM expressing side-population which displays CSC characteristics [9,66]. To determine the changes in the expression of these stemness markers in Huh7, cells were treated with 10 μM **6a** and **13d** for 72 h, and analyzed by flow cytometry. In parallel, cells were also treated with 10 μM Notch-inhibitor DAPT, a known CSC inhibitor [67], and Sorafenib, which is an FDA-approved drug for HCC treatment in clinics, to determine the potency of

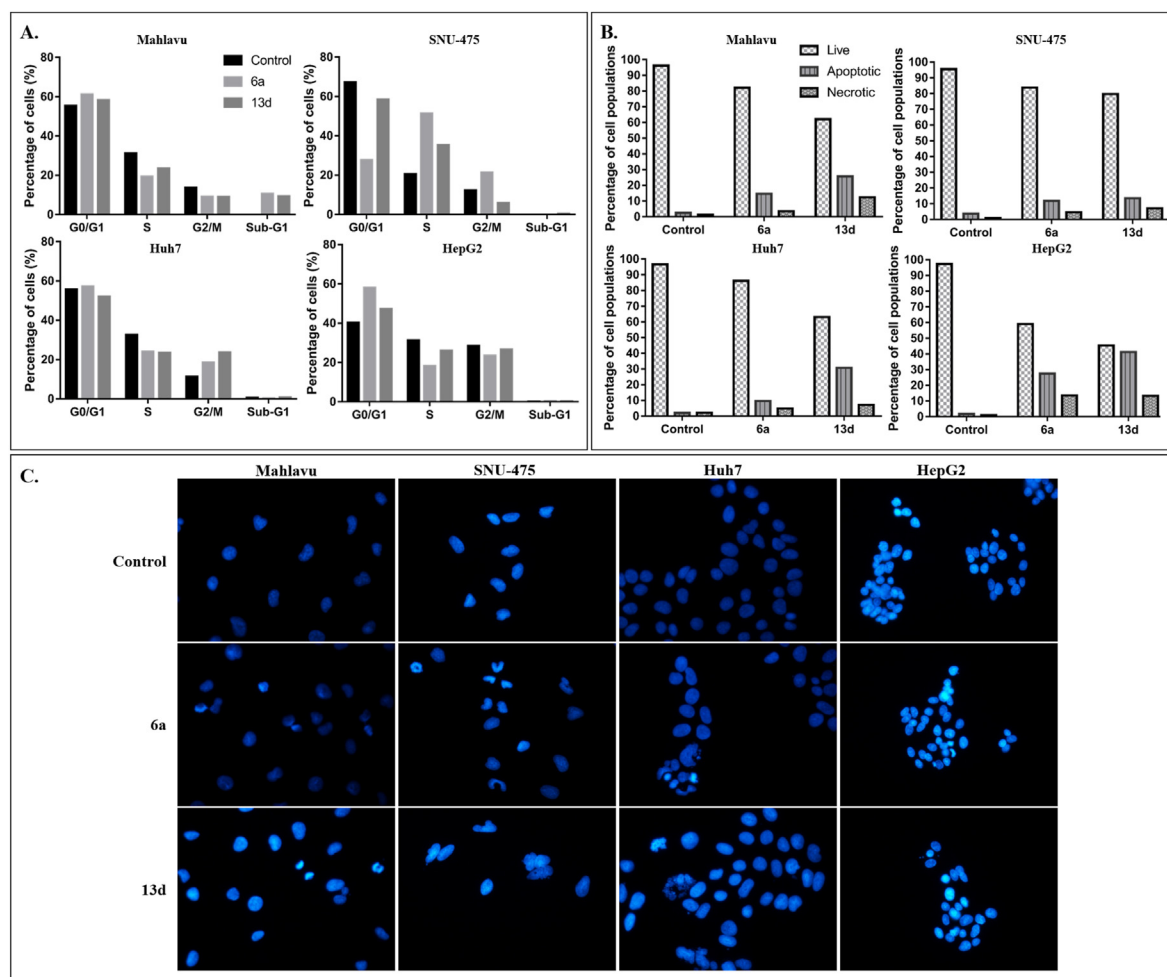


Fig. 4. Compound **6a** and **13d** induced cell cycle arrest and cell death. (A) The effects of compound **6a** and **13d** on cell cycle distributions in Mahlavu, SNU-475, Huh7, and HepG2 cells. Cells were treated with 5 μ M **6a** or **13d** for 48 h and analyzed by flow cytometry based on DNA content. Cell cycle was represented as G0/G1, S, G2/M, and Sub-G1 phases (B) Flow cytometric analysis of Annexin V binding and propidium iodide staining in hepatocellular carcinoma cells undergoing apoptosis. HCC cells were treated with 5 μ M compound **6a** and **13d** and DMSO as control and were analyzed after 72 h. (C) Nuclear morphology was revealed by Hoechst staining under fluorescent microscopy. Apoptotic bodies were seen in **6a** and **13d** treated cells after 48h.

selected compounds on LCSCs. We previously show that Sorafenib causes an increase in LCSC population in Huh7 cells [66]. In parallel with our previous study results, treatment of Huh7 cells with Sorafenib enriched the CD133+/EpCAM+ cells, while compounds **6a** and **13d** led to a significant decrease in the percentage of CD133+/EpCAM+ cells compared with DMSO controls (Fig. 6A). These findings have suggested that the compounds may also be effective against stemness properties of HCC cells.

LCSCs are regulated by different stemness-related genes such as octamer-binding transcription factor 4 (OCT4) and NANOG. OCT4 and NANOG modulate self-renewal and pluripotency of embryonic stem cells (ESCs) [67,68]. Moreover, overexpression of these key regulators of ESC and targets are most frequently related to different types of cancers [69] and many studies showed that these stemness-related genes played a vital role in the development of a malignant tumors, including HCC. NANOG has an active role in self-renewal of LCSCs [70]. It has been reported that OCT4 induces tumor vasculogenesis in LCSCs [71] and OCT4 expression is elevated in chemoresistant HCC cells [72]. In order to understand the effects of compounds on stemness related properties of HCC cells, mRNA and protein levels of stemness-related transcription factors (OCT4 and NANOG) in PTEN deficient Mahlavu and PTEN-adequate Huh7 cells were determined by qRT-PCR and flow cytometry. Mahlavu

and Huh7 cells were treated with compounds **6a** and **13d**, DAPT (as a positive control) and Sorafenib for 72 h. Sorafenib showed a significant increase in mRNA expressions of NANOG and OCT4 genes in both cell lines, whereas compounds **6a** and **13d** resulted in significant reduction in OCT4 and NANOG mRNA levels in Huh7 cells compared to control group. DAPT exhibited similar results with both compounds for OCT4 and NANOG expressions. Compounds **6a**, **13d** and DAPT caused significant reduction in OCT4 mRNA levels, whereas Sorafenib increased the OCT4 gene expression in Mahlavu cells. **13d** treated Mahlavu cells had decreased levels of NANOG gene, whereas Sorafenib treated cells had approximately 10-fold increase in NANOG mRNA levels. **13d** treated Mahlavu cells had slightly decreased levels of NANOG mRNA (Fig. 6B). On the other hand, flow cytometry results revealed that **6a** and **13d** led to a significant decrease in OCT4 and NANOG protein levels in Mahlavu cells and a significant decrease in NANOG protein levels in Huh7 cells. The decrease in gene expression levels of OCT4 in Huh7 cells could not be observed at the protein level, suggesting that changes in NANOG protein levels might be more important in the possible anti-stemness activity of **6a** and **13d**. Sorafenib, which enriches LCSCs caused a significant increase in OCT4 expression, and a significant drop in NANOG expression in Mahlavu cells when compared to DMSO control group for 72 h treatment. (Fig. 6C).

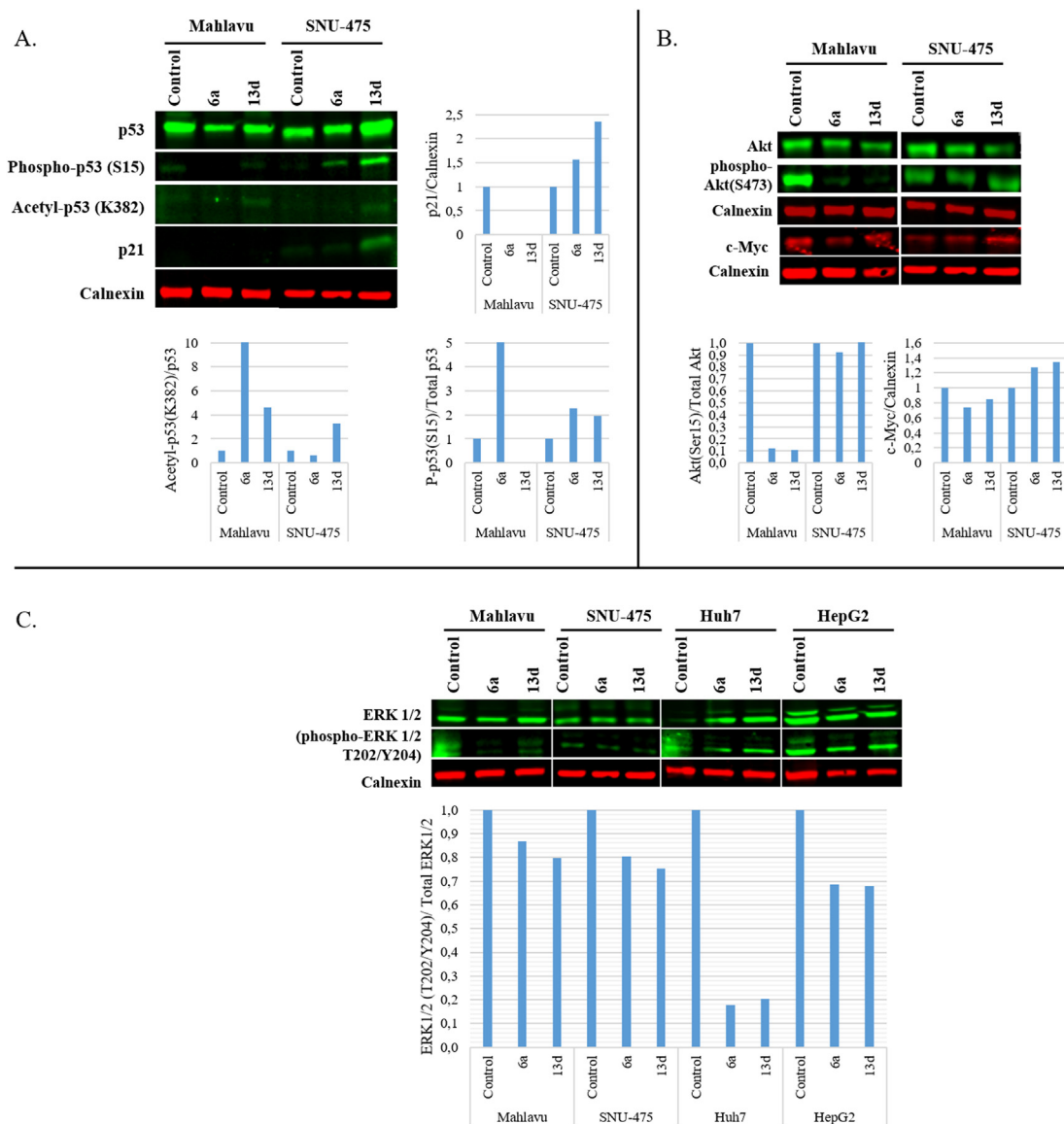


Fig. 5. Western blot analysis of protein levels of Akt, p-Akt, c-Myc, ERK, p-ERK, p53, p-p53, acetyl-p53, and p21 respect to Calnexin (loading control) in **6a** and **13d** treated Mahlavu and SNU-475 cell lines for 72h.

Elevated expression of NANOG in HCC patients was shown to be significantly associated with poor clinical outcomes [68] and recent studies revealed that elevated NANOG expression was related to tumor growth through enriched CSCs [73,74]. Taken together, the expression of stemness related transcription factors, NANOG and OCT4, is important for tumor growth because of liver CSCs. Thus, our results have suggested that the compounds are effective in suppressing the expression of stemness-related transcription factors as well.

Sphere formation is an effective *in vitro* analysis model to functionally study the self-renewal capacity of CSCs [75]. In order to characterize sphere formation capacity of Huh7 cells treated with **6a**, **13d**, DAPT and Sorafenib for 72 h, Huh7 cells were collected and grown in low-attachment plates for 14 days in sphere formation media. After 7 and 14 days, sphere size and amount were measured. **6a**, **13d** and DAPT treated Huh7 cells had smaller sphere size and relatively less sphere count compared to the control group after 7 days. Although Sorafenib treated Huh7 cells had smaller sphere size, its sphere count was higher compared to the control group.

After 14 days, **6a** and **13d** treated Huh7 cells had significantly lower sphere count and smaller average sphere size compared with the control group, whereas Sorafenib treatment caused formation of larger spheres (Fig. 7). These results have once again supported our findings that **6a** and **13d** are not only effective against cancer cells but are also potent Liver CSC growth inhibitors.

3. Conclusion

HCC is one of the most prevalent and the second deadly cancer among other cancer types. Due to the highly heterogeneous nature of HCC, the prognosis of patients is poor and the efficiency of current FDA approved drugs such as sorafenib and regorafenib are still not satisfactory due to acquired-drug resistance. Hence, it is crucial to design and develop novel drug candidates to treat HCC, and overcome mechanisms involved in drug resistance and recurrence of cancer. Here, we explored the anti-cancer and anti-CSC activities of novel isoxazole-piperazine derivatives, exemplified **6a** and **13d**, as potential agents effective against HCC cells as well as liver CSC.

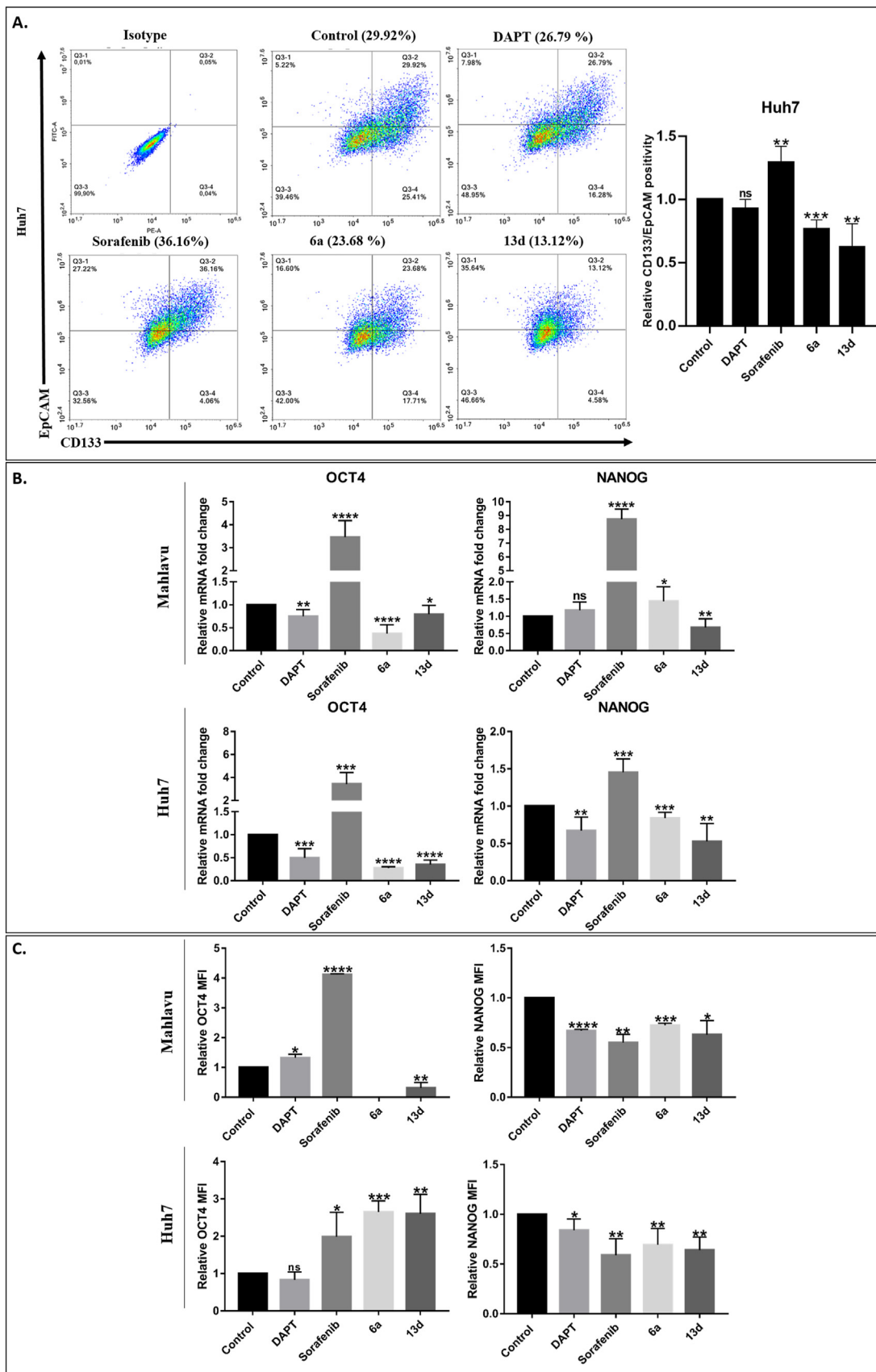


Fig. 6. Effects of compound **6a** and **13d** on stemness characteristics of HCC cells. (A) Representative flow cytometry plots (middle left panel) demonstrating positivity of Huh7 cells for cancer stem cell markers CD133 and EpCAM for 72 h of treatment with 10 μ M DAPT (Notch inhibitor), Sorafenib, **6a**, and **13d** vs control vehicle (DMSO). Cells that survived after each treatment were collected and stained fluorescently with anti-CD133-biotin, anti-biotin-PE and anti-EpCAM-FITC, antibodies. x-axis indicates CD133 positivity, and y-axis

In summary, we initially tested the dose and time dependent growth inhibitory effects of **6a** and **13d** in 4 different HCC cell lines through RT-CES system. Our results revealed that compounds displayed a dose dependent inhibition in cell growth, which was highly correlated with the initial SRB screening results. Further analysis of cell cycle progression and characterization of cell death mechanisms induced by **6a** and **13d** indicated that compounds induced G1 or G2/M arrests which further resulted in apoptotic cell death in HCC cells.

Furthermore, to understand the molecular mechanisms involved in the action of these compounds, analysis of cellular pathways involved in cell cycle progression as well as proliferation and migration of HCC cells were performed. Our results have demonstrated that **6a** and **13d** altered the activity of p53 protein, which is an important transcription factor regulating cell cycle arrest or apoptosis to inhibit tumor progression in mesenchymal HCC cells. Yet the **13d** was found to cause this effect more notably. Additionally, the p53 status in epithelial HCC cells remained unchanged. Similarly, the levels of active Akt protein, which is one of the main components of PI3K/Akt signaling pathway, was shown to decrease in mesenchymal HCC cells upon treatment with **6a** and **13d**. Phosphorylation of ERK1/2 protein that belongs to the Ras/Raf/MEK/ERK pathway (another vital mechanism by which proliferation and survival of HCC cells are regulated) was shown to decrease significantly in mesenchymal cells treated with both **6a** and **13d**. Overall, these results have indicated the potential role of these compounds on the inhibition of proliferation and survival in HCC cells.

Liver CSCs are identified as a population of cells in the tumor microenvironment, capable of re-establishing the tumor by themselves, causing inefficiencies in treatment of HCC patients. Thus, it is also crucial to define the effects of novel compounds on these cell populations to propose stronger drug candidates for HCC. Our results have provided the potential anti-stemness properties of these compounds by different experimental approaches in comparison with Sorafenib and a Notch pathway inhibitor (DAPT). Initially, we have shown that the percentage of LCSCs in Huh7 cells (CD133+/EpCAM+) were significantly decreased upon treatment with **6a** and **13d**. Further analysis of expression levels of stemness-related transcription factors has shown that, these compounds caused a significant reduction in expression of NANOG or OCT4 proteins in Mahlavu and Huh7 cells. Moreover, supportive to these results, **6a** and **13d** resulted in decreased sphere formation capacity in Huh7 cells, which is a well-known character of CSC. To the best of our knowledge, this is the first study to reveal the anti-stemness effects of isoxazole-piperazine derivatives, proposing novel lead compounds for the treatment of HCC with higher efficiencies. Overall, it is worth noting that according to the experimental data obtained in this study, **13d** was found to have more noticeable effects on HCC cells and liver CSCs compared to **6a**.

In conclusion, we have shown that these isoxazole-piperazine derivatives exemplified by **6a** and **13d** potentially inhibit not only proliferation of HCC cells, but also cancer cells with stem-cell like properties. Although our detailed analysis with **6a** and **13d** focuses on liver cancer cells, the initial cytotoxicity of these isoxazole-piperazine hybrids on MCF-7 breast cancer cells makes these compounds candidate for further development against epithelial

cancers.

4. Experimental

4.1. Chemistry

All chemicals were purchased from Sigma Aldrich Chemicals (Sigma Aldrich Corp., St. Louis, MO, USA), Merck Chemicals (Merck KGaA, Darmstadt, Germany), ABCR (abcr GmbH, Karlsruhe, Germany). ¹H and ¹³C NMR spectra were recorded in CDCl₃ or DMSO-*d*₆ on a Varian Mercury 400 MHz spectrometer, Bruker Avance Neo 500 MHz or Bruker Ultrashield 300 MHz using tetramethylsilane as the internal standard. All chemical shifts were recorded as δ (ppm), and coupling constants are reported as Hertz. High resolution mass spectra data (HRMS) were collected using Waters LCT Premier XE Mass Spectrometer (high sensitivity orthogonal acceleration time-of-flight) operating in ESI (+) or ESI (-) method, also coupled to an AQUITY Ultra Performance Liquid Chromatography system (Waters Corporation) using a UV detector monitoring at 254 nm. Purity for all final compounds was >95%, according to the UPLC-MS method using (A) water + 0.1% Formic Acid and (B) acetonitrile + 0.1% Formic Acid; flow rate = 0.3 mL/min, Column: Aquity BEH C18 column (2.1 \times 100 mm, 1.7 mm). All microwave irradiation experiments were carried out in a Biotage Initiator + microwave apparatus with Biotage sealed microwave vials. Flash chromatography on silica gel was performed on RediSep prepacked disposable silica gel columns using Teledyne Isco Combiflash. Melting points of the synthesized compounds were determined by an SMP50 automatic melting point apparatus (Stuart, Staffordshire, ST15 OSA, UK). FTIR spectra were recorded on a PerkinElmer Spectrum 400 FTIR/FTNIR spectrometer equipped with a Universal ATR Sampling Accessory. Elemental analyses were performed with a LECO-932 (C, H, N, S-Elemental Analyzer) and the results were within \pm 0.4% of the theoretical values. Compounds **1–3** were synthesized according to the previously published procedures [34]. Experimental data for all intermediate compounds can be found in Supporting Information.

4.1.1. Synthesis of Compounds **6a–t**, Compounds **7a–n**, **13a–d**, **14**, **15**

The mixture of the appropriate bromide (**5a–t**, **12 c–d**), or chloride derivative (**12a–b**) (0.5 mmol, 1 eq), appropriate amine (0.6 mmol, 1.2 eq) and DIEA (1 mmol, 2 eq) in DMF (2 ml) was heated by microwave irradiation at 80 °C for 20 min. Then, it was poured into ice-water and formed precipitate was filtrated. The crude product was purified by flash chromatography.

4.1.1.1. 5-(4-(Benzyloxy)phenyl)-3-((4-(trifluoromethyl)benzyl)piperazin-1-yl)methylisoxazole (**6a**). Purified by flash column chromatography (0% \rightarrow 10% MeOH in DCM). Yield 63.7%; mp 137.7–137.9 °C. IR (ATR) ν : 3098, 2947, 2805, 1613, 1328, 1246, 1117, 748 cm⁻¹. ¹H NMR (500 MHz, CDCl₃): δ _H 2.53 (br s, 4H, piperazine), 2.60 (br s, 4H, piperazine), 3.58 (s, 2H, -N-CH₂-Ar), 3.66 (s, 2H, -N-CH₂-isoxazole), 5.14 (s, 2H, -O-CH₂-Ar), 6.45 (s, 1H, isoxazole-H), 7.06 (d, *J* = 8.9 Hz, 2H, Ar-H), 7.35–7.39 (m, 1H, Ar-H), 7.41–7.47 (m, 6H, Ar-H), 7.59 (d, *J* = 8.0 Hz, 2H, Ar-H), 7.73 (d, *J* = 8.9 Hz, 2H, Ar-H). ¹³C NMR (125 MHz, CDCl₃): δ _C 169.87, 161.77, 160.21, 142.47, 136.42, 129.33 (q, ²*J*_{C-F} = 32.1 Hz), 129.20, 128.69, 128.19, 127.48, 127.40, 125.17 (q, ³*J*_{C-F} = 3.7 Hz), 124.48 (q, ¹*J*_{C-F} = 270.0 Hz), 120.61,

indicates EpCAM positivity. Lower-left quadrant, CD133-/EpCAM-; Upper-left quadrant, CD133-/EpCAM+; Lower-right quadrant, CD133+/EpCAM-; upper-right quadrant, CD133+/EpCAM+. Each treatment was compared to its corresponding DMSO control to define the changes in percentage of double positive population. DAPT was used as positive control for CSC inhibition. Bar graph (middle right panel) indicates relative CD133/EpCAM positivity with respect to control group. Experiments were performed in 3 biological replicates at different times. (B) Bar graphs illustrating relative expression of OCT4 and NANOG in Huh7 and Mahlavu cell lines with 10 μ M Sorafenib, DAPT, **6a**, and **13d** treatment for 72h by qRT-PCR Housekeeping gene GAPDH was used as internal control. (C) Relative Mean fluorescence intensity (MFI) values of 10 μ M **6a**, **13d**, Sorafenib, DAPT and control treated Mahlavu and Huh7 cells in terms of expression of OCT4 and NANOG are determined by flow cytometry. Experiments were performed in 3 biological replicates at different times.

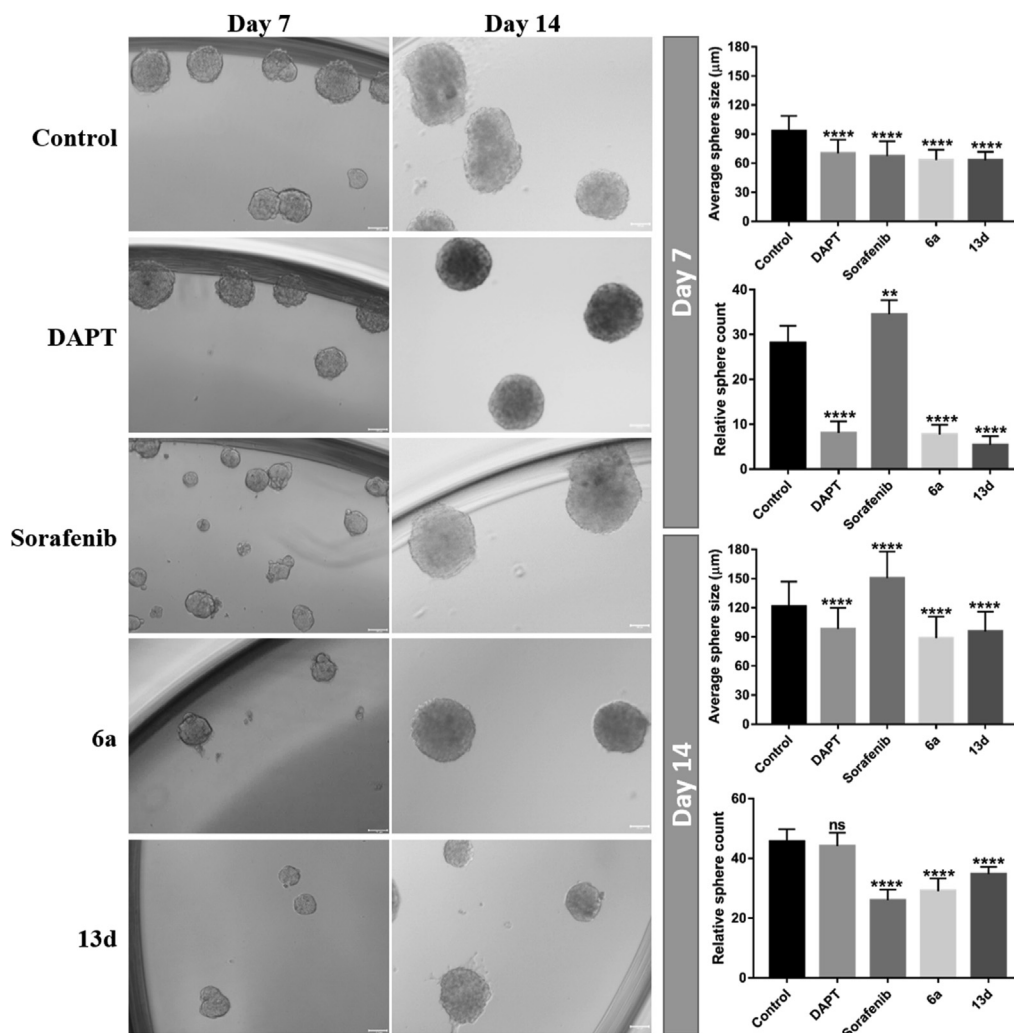


Fig. 7. Compound **6a** and **13d** inhibits sphere formation on Huh7 cells. (A) Representative 10X microscopic images of sphere formation generated after 7 days and 14 days treated with 10 μ M DAPT, Sorafenib, **6a** and **13d**. Scale bar: 100 μ m. (B) Bar graphs comparing the number of spheres for each treatment group and sphere size relative to DMSO control. Quantification of sphere formation assay revealed that **6a** and **13d** reduced the sphere formation ability of Huh7 cells.

115.29, 98.34, 70.12, 62.37, 53.40, 53.08, 52.99. HRMS (m/z) $[M+H]^+$ calcd for $C_{29}H_{29}F_3N_3O_2$: 508.2212, found: 508.2192. Anal. Calcd for $C_{29}H_{28}F_3N_3O_2$: C, 68.62; H, 5.56; N, 8.28. Found: C, 68.29; H, 5.39; N, 8.26.

4.1.1.2. 5-(4-((2-Methylbenzyl)oxy)phenyl)-3-((4-(4-(trifluoromethyl)benzyl)piperazin-1-yl)methyl)isoxazole (**6b**). Purified by flash column chromatography (0% \rightarrow 10% MeOH in DCM). Yield 80%; mp 124.6–126.2 $^{\circ}$ C. IR (ATR) ν : 3117, 2950, 2801, 1615, 1326, 1242, 1130, 746 cm^{-1} . 1H NMR (400 MHz, $CDCl_3$): δ_H 2.38 (s, 3H, Ar- CH_3), 2.50 (br s, 4H, piperazine), 2.57 (br s, 4H, piperazine), 3.56 (s, 2H, -N- CH_2 -Ar), 3.64 (s, 2H, -N- CH_2 -isoxazole), 5.08 (s, 2H, -O- CH_2 -Ar), 6.43 (s, 1H, isoxazole-H), 7.05 (d, J = 8.6 Hz, 2H, Ar-H), 7.22–7.27 (m, 3H, Ar-H), 7.39–7.45 (m, 3H, Ar-H), 7.56 (d, J = 8.0 Hz, 2H, Ar-H), 7.71 (d, J = 8.6 Hz, 2H, Ar-H). ^{13}C NMR (100 MHz, $CDCl_3$): δ 169.88, 161.77, 160.34, 142.46, 136.71, 134.23, 130.52, 129.34 (q, $^2J_{C-F}$ = 31.5 Hz), 129.18, 128.63, 128.50, 127.41, 126.11, 125.16 (q, $^3J_{C-F}$ = 3.8 Hz), 124.25 (q, $^1J_{C-F}$ = 269.9 Hz), 120.61, 115.19, 98.32, 68.74, 62.36, 53.40, 53.08, 52.98, 18.90. HRMS (m/z) $[M+H]^+$ calcd for $C_{30}H_{31}F_3N_3O_2$: 522.2368, found: 522.2374.

4.1.1.3. 5-(4-((3-Methylbenzyl)oxy)phenyl)-3-((4-(4-(trifluoromethyl)benzyl)piperazin-1-yl)methyl)isoxazole (**6c**). Purified by flash column chromatography (0% \rightarrow 10% MeOH in DCM). Yield 74.5%; mp 131.5–133.4 $^{\circ}$ C. IR (ATR) ν : 3115, 2943, 2799, 1614, 1328, 1247, 1152, 1120, 1007, 787 cm^{-1} . 1H NMR (400 MHz, $CDCl_3$): δ_H 2.38 (s, 3H, Ar- CH_3), 2.50 (br s, 4H, piperazine), 2.57 (br s, 4H, piperazine), 3.56 (s, 2H, -N- CH_2 -Ar), 3.63 (s, 2H, -N- CH_2 -isoxazole), 5.07 (s, 2H, -O- CH_2 -Ar), 6.43 (s, 1H, isoxazole-H), 7.03 (d, J = 9.2 Hz, 2H, Ar-H), 7.15 (d, J = 7.6 Hz, 1H, Ar-H), 7.22–7.31 (m, 3H, Ar-H), 7.43 (d, J = 7.6 Hz, 2H, Ar-H), 7.56 (d, J = 7.6 Hz, 2H, Ar-H), 7.70 (d, J = 9.2 Hz, 2H, Ar-H). ^{13}C NMR (100 MHz, $CDCl_3$): δ_C 168.88, 161.76, 160.27, 142.45, 138.41, 136.30, 129.33 (q, $^2J_{C-F}$ = 30.5 Hz), 129.18, 128.95, 128.58, 128.22, 127.37, 125.15 (q, $^3J_{C-F}$ = 3.8 Hz), 124.58, 124.25 (q, $^1J_{C-F}$ = 269.8 Hz), 120.55, 115.26, 98.29, 70.18, 62.35, 53.39, 53.07, 52.98, 21.41. HRMS (m/z) $[M+H]^+$ calcd for $C_{30}H_{31}F_3N_3O_2$: 522.2368, found: 522.2365. Anal. Calcd for $C_{30}H_{30}F_3N_3O_2$: C, 69.08; H, 5.80; N, 8.06. Found: C, 69.00; H, 5.63; N, 8.16.

4.1.1.4. 5-(4-((4-Methylbenzyl)oxy)phenyl)-3-((4-(4-(trifluoromethyl)benzyl)piperazin-1-yl)methyl)isoxazole (**6d**). Purified by flash column chromatography (0% \rightarrow 10% MeOH in

DCM). Yield 39.0%; mp 159.2–160.9 °C. IR (ATR) ν : 3113, 2944, 2801, 1615, 1326, 1245, 1157, 1133 cm^{-1} . ^1H NMR (400 MHz, CDCl_3): δ_{H} 2.36 (s, 3H, Ar- CH_3), 2.50 (br s, 4H, piperazine), 2.57 (br s, 4H, piperazine), 3.56 (s, 2H, -N- CH_2 -Ar), 3.63 (s, 2H, -N- CH_2 -isoxazole), 5.07 (s, 2H, -O- CH_2 -Ar), 6.42 (s, 1H, isoxazole-H), 7.03 (d, $J = 8.8$ Hz, 2H, Ar-H), 7.20 (d, $J = 8.0$ Hz, 2H, Ar-H), 7.32 (d, $J = 8.0$ Hz, 2H, Ar-H), 7.43 (d, $J = 7.8$ Hz, 2H, Ar-H), 7.56 (d, $J = 7.8$ Hz, 2H, Ar-H), 7.69 (d, $J = 8.8$ Hz, 2H, Ar-H). ^{13}C NMR (100 MHz, CDCl_3): δ_{C} 169.89, 161.70, 160.26, 142.39, 138.00, 133.34, 129.34, 129.32 (q, $^2J_{\text{C-F}} = 31.5$ Hz), 129.18, 127.60, 127.35, 124.23 (q, $^1J_{\text{C-F}} = 270.5$ Hz), 125.15 (q, $^3J_{\text{C-F}} = 3.5$ Hz), 124.23, 120.47, 115.25, 98.27, 70.04, 62.32, 53.36, 53.04, 52.94, 21.18. HRMS (m/z) $[\text{M}+\text{H}]^+$ calcd for $\text{C}_{30}\text{H}_{31}\text{F}_3\text{N}_3\text{O}_2$: 522.2368, found: 522.2363. Anal. Calcd for $\text{C}_{30}\text{H}_{30}\text{F}_3\text{N}_3\text{O}_2$: C, 69.08; H, 5.80; N, 8.06. Found: C, 69.45; H, 5.86; N, 7.87.

4.1.1.5. 5-(4-((3,5-Dimethylbenzyl)oxy)phenyl)-3-((4-(4-(trifluoromethyl)benzyl)piperazin-1-yl)methyl)isoxazole (**6e**). Purified by flash column chromatography (0% \rightarrow 10% MeOH in DCM). Yield 86.0%; mp 111.8–112.8 °C. IR (ATR) ν : 3027, 2950, 2801, 1614, 1321, 1245, 1128, 1064, 799 cm^{-1} . ^1H NMR (400 MHz, CDCl_3): δ_{H} 2.33 (s, 6H, Ar- CH_3), 2.49 (br s, 4H, piperazine), 2.57 (br s, 4H, piperazine), 3.56 (s, 2H, -N- CH_2 -Ar), 3.63 (s, 2H, -N- CH_2 -isoxazole), 5.03 (s, 2H, -O- CH_2 -Ar), 6.42 (s, 1H, isoxazole-H), 6.98 (s, 1H, Ar-H), 7.02–7.04 (m, 4H, Ar-H), 7.43 (d, $J = 7.6$ Hz, 2H, Ar-H), 7.56 (d, $J = 7.6$ Hz, 2H, Ar-H), 7.70 (d, $J = 8.8$ Hz, 2H, Ar-H). ^{13}C NMR (100 MHz, CDCl_3): δ_{C} 169.91, 161.77, 160.35, 142.46, 138.32, 136.24, 129.86, 129.70 (q, $^2J_{\text{C-F}} = 31.5$ Hz), 129.18, 127.38, 125.39, 125.16 (q, $^3J_{\text{C-F}} = 3.8$ Hz), 124.20 (q, $^1J_{\text{C-F}} = 270.0$ Hz), 120.50, 115.25, 98.28, 70.26, 62.36, 53.40, 53.08, 52.99, 21.29. HRMS (m/z) $[\text{M}+\text{H}]^+$ calcd for $\text{C}_{31}\text{H}_{32}\text{F}_3\text{N}_3\text{O}_2$: 536.2525, found: 536.2534. Anal. Calcd for $\text{C}_{31}\text{H}_{31}\text{F}_3\text{N}_3\text{O}_2$: C, 69.65; H, 5.84; N, 7.86. Found: C, 69.56; H, 6.00; N, 8.06.

4.1.1.6. 5-(4-((2-Chlorobenzyl)oxy)phenyl)-3-((4-(4-(trifluoromethyl)benzyl)piperazin-1-yl)methyl)isoxazole (**6f**). Purified by flash column chromatography (0% \rightarrow 10% MeOH in DCM). Yield 59.0%; mp 127.9–128.5 °C. IR (ATR) ν : 3130, 2943, 2805, 1614, 1325, 1246, 1117, 765 cm^{-1} . ^1H NMR (400 MHz, CDCl_3): δ_{H} 2.50 (br s, 4H, piperazine), 2.57 (br s, 4H, piperazine), 3.56 (s, 2H, -N- CH_2 -Ar), 3.64 (s, 2H, -N- CH_2 -isoxazole), 5.22 (s, 2H, -O- CH_2 -Ar), 6.44 (s, 1H, isoxazole-H), 7.04 (d, $J = 8.6$ Hz, 2H, Ar-H), 7.27–7.32 (m, 2H, Ar-H), 7.40–7.44 (m, 3H, Ar-H), 7.53–7.57 (m, 3H, Ar-H), 7.71 (d, $J = 8.6$ Hz, 2H, Ar-H). ^{13}C NMR (100 MHz, CDCl_3): δ_{C} 169.79, 161.79, 159.91, 142.47, 134.16, 132.66, 129.49, 129.21, 128.19, 128.77, 127.45, 127.04, 125.17 (q, $^3J_{\text{C-F}} = 3.6$ Hz), 124.25 (q, $^1J_{\text{C-F}} = 270.0$ Hz), 120.86, 115.28, 98.42, 67.22, 62.36, 53.39, 53.08, 52.99. HRMS (m/z) $[\text{M}+\text{H}]^+$ calcd for $\text{C}_{29}\text{H}_{27}\text{ClF}_3\text{N}_3\text{O}_2$: 542.1822, found: 542.1813. Anal. Calcd for $\text{C}_{29}\text{H}_{27}\text{ClF}_3\text{N}_3\text{O}_2$: C, 64.26; H, 5.02; N, 7.75. Found: C, 64.25; H, 4.94; N, 7.61.

4.1.1.7. 5-(4-((3-Chlorobenzyl)oxy)phenyl)-3-((4-(4-(trifluoromethyl)benzyl)piperazin-1-yl)methyl)isoxazole (**6g**). Purified by flash column chromatography (0% \rightarrow 10% MeOH in DCM). Yield 80.1%; mp 117.4–118.0 °C. IR (ATR) ν : 3136, 2946, 2809, 1614, 1331, 1264, 1122, 835 cm^{-1} . ^1H NMR (400 MHz, CDCl_3): δ_{H} 2.50 (br s, 4H, piperazine), 2.57 (br s, 4H, piperazine), 3.56 (s, 2H, -N- CH_2 -Ar), 3.63 (s, 2H, -N- CH_2 -isoxazole), 5.09 (s, 2H, -O- CH_2 -Ar), 6.43 (s, 1H, isoxazole-H), 7.02 (d, $J = 9.0$ Hz, 2H, Ar-H), 7.31–7.32 (m, 3H, Ar-H), 7.42–7.44 (m, 3H, Ar-H), 7.56 (d, $J = 8.0$ Hz, 2H, Ar-H), 7.71 (d, $J = 9.0$ Hz, 2H, Ar-H). ^{13}C NMR (100 MHz, CDCl_3): δ_{C} 169.73, 161.79, 159.84, 142.4, 138.48, 134.63, 129.95, 129.33 (q, $^2J_{\text{C-F}} = 30.7$ Hz), 129.18, 128.30, 127.44, 127.41, 125.33, 125.19 (q, $^3J_{\text{C-F}} = 3.6$ Hz), 124.24 (q, $^1J_{\text{C-F}} = 269.9$ Hz), 120.87, 115.24, 98.43, 69.22, 62.35, 53.37, 53.07, 52.97. HRMS (m/z) $[\text{M}+\text{H}]^+$ calcd for

$\text{C}_{29}\text{H}_{28}\text{ClF}_3\text{N}_3\text{O}_2$: 542.1822, found: 542.1836. Anal. Calcd for $\text{C}_{29}\text{H}_{27}\text{ClF}_3\text{N}_3\text{O}_2$: C, 64.26; H, 5.02; N, 7.75. Found: C, 64.38; H, 4.99; N, 7.71.

4.1.1.8. 5-(4-((4-Chlorobenzyl)oxy)phenyl)-3-((4-(4-(trifluoromethyl)benzyl)piperazin-1-yl)methyl)isoxazole (**6h**). Purified by flash column chromatography (0% \rightarrow 10% MeOH in DCM). Yield 62.1%; mp 158.8–159.0 °C. IR (ATR) ν : 3136, 2943, 2800, 1615, 1322, 1244, 1134, 1009, 800 cm^{-1} . ^1H NMR (400 MHz, CDCl_3): δ_{H} 2.50 (br s, 4H, piperazine), 2.57 (br s, 4H, piperazine), 3.55 (s, 2H, -N- CH_2 -Ar), 3.63 (s, 2H, -N- CH_2 -isoxazole), 5.07 (s, 2H, -O- CH_2 -Ar), 6.43 (s, 1H, isoxazole-H), 7.01 (d, $J = 9.0$ Hz, 2H, Ar-H), 7.36 (s, 4H, Ar-H), 7.43 (d, $J = 8.0$ Hz, 2H, Ar-H), 7.56 (d, $J = 8.0$ Hz, 2H, Ar-H), 7.70 (d, $J = 9.0$ Hz, 2H, Ar-H). ^{13}C NMR (100 MHz, CDCl_3): δ_{C} 169.74, 161.75, 159.89, 142.40, 134.89, 133.99, 129.33 (q, $^2J_{\text{C-F}} = 32.0$ Hz), 129.17, 128.85, 128.75, 127.41, 125.15 (q, $^3J_{\text{C-F}} = 3.9$ Hz), 124.23 (q, $^1J_{\text{C-F}} = 270.1$ Hz), 120.79, 115.23, 98.40, 69.29, 63.33, 53.36, 53.05, 52.94. HRMS (m/z) $[\text{M}+\text{H}]^+$ calcd for $\text{C}_{29}\text{H}_{28}\text{ClF}_3\text{N}_3\text{O}_2$: 542.1822, found: 542.1827.

4.1.1.9. 2-((4-(3-((4-(4-(Trifluoromethyl)benzyl)piperazin-1-yl)methyl)isoxazol-5-yl)phenoxy)methyl)benzonitrile (**6i**). Purified by flash column chromatography (0% \rightarrow 10% MeOH in DCM). Yield 75.9%; mp 148.9–151.2 °C. IR (ATR) ν : 3132, 2939, 2802, 2230, 1615, 1326, 1246, 1115, 1100, 774 cm^{-1} . ^1H NMR (400 MHz, CDCl_3): δ_{H} 2.50 (br s, 4H, piperazine), 2.57 (br s, 4H, piperazine), 3.56 (s, 2H, -N- CH_2 -Ar), 3.64 (s, 2H, -N- CH_2 -isoxazole), 5.31 (s, 2H, -O- CH_2 -Ar), 6.45 (s, 1H, isoxazole-H), 7.07 (d, $J = 9.0$ Hz, 2H, Ar-H), 7.42–7.48 (m, 3H, Ar-H), 7.56 (d, $J = 7.6$ Hz, 2H, Ar-H), 7.62–7.69 (m, 3H, Ar-H), 7.73 (d, $J = 9.0$ Hz, 2H, Ar-H). ^{13}C NMR (100 MHz, CDCl_3): δ_{C} 169.64, 161.83, 159.51, 142.48, 142.46, 140.01, 133.15, 132.99, 129.34 (q, $^2J_{\text{C-F}} = 29.5$ Hz), 129.19, 128.46, 127.52, 125.16 (q, $^3J_{\text{C-F}} = 3.9$ Hz), 124.26 (q, $^1J_{\text{C-F}} = 270.6$ Hz), 121.28, 116.98, 115.32, 111.24, 98.59, 67.63, 62.36, 53.38, 53.09, 52.99. HRMS (m/z) $[\text{M}+\text{H}]^+$ calcd for $\text{C}_{30}\text{H}_{28}\text{F}_3\text{N}_4\text{O}_2$: 533.2164, found: 533.2161. Anal. Calcd for $\text{C}_{30}\text{H}_{27}\text{F}_3\text{N}_4\text{O}_2$: C, 67.66; H, 5.11; N, 10.52. Found: C, 67.65; H, 5.01; N, 10.81.

4.1.1.10. 3-((4-(3-((4-(4-(Trifluoromethyl)benzyl)piperazin-1-yl)methyl)isoxazol-5-yl)phenoxy)methyl)benzonitrile (**6j**). Purified by flash column chromatography (0% \rightarrow 10% MeOH in DCM). Yield 85.0%; mp 164.9–166.0 °C. IR (ATR) ν : 3071, 2952, 2810, 2229, 1616, 1324, 1249, 1118, 799 cm^{-1} . ^1H NMR (400 MHz, CDCl_3): δ_{H} 2.50 (br s, 4H, piperazine), 2.57 (br s, 4H, piperazine), 3.56 (s, 2H, -N- CH_2 -Ar), 3.64 (s, 2H, -N- CH_2 -isoxazole), 5.15 (s, 2H, -O- CH_2 -Ar), 6.45 (s, 1H, isoxazole-H), 7.03 (d, $J = 8.8$ Hz, 2H, Ar-H), 7.44 (d, $J = 8.0$ Hz, 2H, Ar-H), 7.52 (t, $J = 7.6$ Hz, 1H, Ar-H), 7.56 (d, $J = 8.0$ Hz, 2H, Ar-H), 7.64–7.69 (m, 2H, Ar-H), 7.73 (d, $J = 8.8$ Hz, 2H, Ar-H), 7.75 (s, 1H, Ar-H). ^{13}C NMR (100 MHz, CDCl_3): δ_{C} 169.59, 161.82, 159.52, 142.43, 138.09, 131.75, 131.45, 130.69, 129.50, 129.34 (q, $^2J_{\text{C-F}} = 32.0$ Hz), 129.18, 127.51, 125.15 (q, $^3J_{\text{C-F}} = 3.9$ Hz), 124.30 (q, $^1J_{\text{C-F}} = 270.0$ Hz), 121.16, 118.52, 115.20, 112.90, 98.56, 68.72, 62.34, 53.36, 53.07, 52.96. HRMS (m/z) $[\text{M}+\text{H}]^+$ calcd for $\text{C}_{30}\text{H}_{28}\text{F}_3\text{N}_4\text{O}_2$: 533.2164, found: 533.2158. Anal. Calcd for $\text{C}_{30}\text{H}_{27}\text{F}_3\text{N}_4\text{O}_2 \cdot 0.1 \text{CH}_2\text{Cl}_2$: C, 66.82; H, 5.07; N, 10.36. Found: C, 66.67; H, 5.05; N, 10.75.

4.1.1.11. 4-((4-(3-((4-(4-(Trifluoromethyl)benzyl)piperazin-1-yl)methyl)isoxazol-5-yl)phenoxy)methyl)benzonitrile (**6k**). Purified by flash column chromatography (0% \rightarrow 10% MeOH in DCM). Yield 75.3%; mp 140.2–141.8 °C. IR (ATR) ν : 3046, 2917, 2820, 2236, 1615, 1319, 1248, 1114, 1101, 824 cm^{-1} . ^1H NMR (400 MHz, CDCl_3): δ_{H} 2.50 (br s, 4H, piperazine), 2.57 (br s, 4H, piperazine), 3.56 (s, 2H, -N- CH_2 -Ar), 3.63 (s, 2H, -N- CH_2 -isoxazole), 5.17 (s, 2H, -O- CH_2 -Ar), 6.44 (s, 1H, isoxazole-H), 7.01 (d, $J = 8.4$ Hz, 2H, Ar-H), 7.43 (d, $J = 8.0$ Hz, 2H, Ar-H), 7.54–7.56 (m, 4H, Ar-H), 7.68–7.73 (m, 4H, Ar-H). ^{13}C

NMR (100 MHz, CDCl₃): δ_C 169.78, 162.02, 159.73, 142.62, 142.05, 132.69, 129.54 (q, $^2J_{C-F}$ = 31.5 Hz), 129.38, 127.77, 127.71, 125.36 (q, $^3J_{C-F}$ = 3.8 Hz), 124.44 (q, $^1J_{C-F}$ = 270.0 Hz), 121.37, 118.77, 115.41, 112.18, 98.76, 69.17, 62.55, 53.57, 53.28, 53.16. HRMS (m/z) [M+H]⁺ calcd for C₃₀H₂₈F₃N₄O₂: 533.2164, found: 533.2177. Anal. Calcd for C₃₀H₂₇F₃N₄O₂: C, 67.66; H, 5.11; N, 10.52. Found: C, 67.60; H, 4.81; N, 10.25.

4.1.1.12. 5-(4-((2-Fluorobenzyl)oxy)phenyl)-3-((4-(4-(trifluoromethyl)benzyl)piperazin-1-yl)methyl)isoxazole (6l).

Purified by flash column chromatography (0% → 10% MeOH in DCM). Yield 79.5%; mp 137.6–138.0 °C. IR (ATR) ν : 3124, 2944, 2817, 1614, 1454, 1324, 1247, 1116, 1064, 806 cm⁻¹. ¹H NMR (400 MHz, CDCl₃): δ_H 2.50 (br s, 4H, piperazine), 2.57 (br s, 4H, piperazine), 3.56 (s, 2H, -N-CH₂-Ar), 3.63 (s, 2H, -N-CH₂-isoxazole), 5.18 (s, 2H, -O-CH₂-Ar), 6.43 (s, 1H, isoxazole-H), 7.05 (d, J = 8.8 Hz, 2H, Ar-H), 7.07–7.13 (m, 1H, Ar-H), 7.15–7.19 (m, 1H, Ar-H), 7.30–7.36 (m, 1H, Ar-H), 7.43 (d, J = 7.6 Hz, 2H, Ar-H), 7.50 (td, J = 7.6 Hz, 1.6 Hz, 1H, Ar-H), 7.55 (d, J = 7.6 Hz, 2H, Ar-H), 7.72 (d, J = 8.8 Hz, 2H, Ar-H). ¹³C NMR (100 MHz, CDCl₃): δ_C 169.79, 161.77, 160.46 (d, $^1J_{C-F}$ = 245.5 Hz), 159.94, 142.45, 129.95 (d, $^3J_{C-F}$ = 8.4 Hz), 129.67 (d, $^3J_{C-F}$ = 3.9 Hz), 129.33 (q, $^2J_{C-F}$ = 30.7 Hz), 129.18, 127.41, 125.15 (q, $^3J_{C-F}$ = 3.6 Hz), 124.33 (d, $^4J_{C-F}$ = 3.9 Hz), 124.33 (d, $^4J_{C-F}$ = 3.9 Hz), 124.24 (q, $^1J_{C-F}$ = 270.6 Hz), 123.59 (d, $^2J_{C-F}$ = 14.1 Hz), 120.80, 115.44 (d, $^2J_{C-F}$ = 20.5 Hz), 115.21, 98.39, 63.79 (d, $^3J_{C-F}$ = 4.4 Hz), 62.35, 53.38, 53.07, 52.98. HRMS (m/z) [M+H]⁺ calcd for C₂₉H₂₈F₄N₃O₂: 526.2118, found: 526.2123. Anal. Calcd for C₂₉H₂₇F₄N₃O₂: C, 66.28; H, 5.18; N, 8.00. Found: C, 66.19; H, 5.15; N, 8.33.

4.1.1.13. 5-(4-((3-Fluorobenzyl)oxy)phenyl)-3-((4-(4-(trifluoromethyl)benzyl)piperazin-1-yl)methyl)isoxazole (6m).

Purified by flash column chromatography (0% → 10% MeOH in DCM). Yield 71.2%; mp 112.6–113.1 °C. IR (ATR) ν : 3126, 2946, 2803, 1614, 1325, 1247, 1117, 1065, 766 cm⁻¹. ¹H NMR (400 MHz, CDCl₃): δ_H 2.50 (br s, 4H, piperazine), 2.57 (br s, 4H, piperazine), 3.56 (s, 2H, -N-CH₂-Ar), 3.63 (s, 2H, -N-CH₂-isoxazole), 5.11 (s, 2H, -O-CH₂-Ar), 6.43 (s, 1H, isoxazole-H), 7.00–7.04 (m, 3H, Ar-H), 7.15–7.21 (m, 2H, Ar-H), 7.33–7.39 (m, 1H, Ar-H), 7.43 (d, J = 7.8 Hz, 2H, Ar-H), 7.56 (d, J = 7.8 Hz, 2H, Ar-H), 7.70 (d, J = 8.8 Hz, 2H, Ar-H). ¹³C NMR (100 MHz, CDCl₃): δ_C 169.74, 163.00 (d, $^1J_{C-F}$ = 246.1 Hz), 161.77, 159.86, 142.43, 139.01 (d, $^3J_{C-F}$ = 6.8 Hz), 130.23 (d, $^3J_{C-F}$ = 7.6 Hz), 129.33 (q, $^2J_{C-F}$ = 30.5 Hz), 129.18, 127.43, 125.15 (q, $^3J_{C-F}$ = 3.8 Hz), 124.24 (q, $^1J_{C-F}$ = 269.8 Hz), 122.69 (d, $^4J_{C-F}$ = 2.3 Hz), 120.84, 115.24, 115.02 (d, $^2J_{C-F}$ = 21.3 Hz), 114.21 (d, $^2J_{C-F}$ = 22.1 Hz), 98.42, 69.24 (d, $^4J_{C-F}$ = 1.5 Hz), 62.34, 53.37, 53.06, 52.96. HRMS (m/z) [M+H]⁺ calcd for C₂₉H₂₈F₄N₃O₂: 526.2118, found: 526.2113. Anal. Calcd for C₂₉H₂₇F₄N₃O₂: C, 66.28; H, 5.18; N, 8.00. Found: C, 66.36; H, 5.05; N, 8.39.

4.1.1.14. 5-(4-((4-Fluorobenzyl)oxy)phenyl)-3-((4-(4-(trifluoromethyl)benzyl)piperazin-1-yl)methyl)isoxazole (6n).

Purified by flash column chromatography (0% → 10% MeOH in DCM). Yield 84.2%; mp 155.7–156.1 °C. IR (ATR) ν : 3050, 2945, 2806, 1614, 1512, 1226, 1115, 820 cm⁻¹. ¹H NMR (400 MHz, CDCl₃): δ_H 2.50 (br s, 4H, piperazine), 2.57 (br s, 4H, piperazine), 3.56 (s, 2H, -N-CH₂-Ar), 3.63 (s, 2H, -N-CH₂-isoxazole), 5.06 (s, 2H, -O-CH₂-Ar), 6.43 (s, 1H, isoxazole-H), 7.02 (d, J = 8.8 Hz, 2H, Ar-H), 7.08 (t, J = 8.6 Hz, 2H, Ar-H), 7.39–7.44 (m, 4H, Ar-H), 7.56 (d, J = 7.6 Hz, 2H, Ar-H), 7.70 (d, J = 8.8 Hz, 2H, Ar-H). ¹³C NMR (100 MHz, CDCl₃): δ_C 169.77, 162.59 (d, $^1J_{C-F}$ = 245.6 Hz), 161.74, 159.99, 142.40, 132.15 (d, $^4J_{C-F}$ = 3.2 Hz), 129.34 (d, $^3J_{C-F}$ = 8.3 Hz), 129.32 (q, $^2J_{C-F}$ = 32.0 Hz), 129.18, 127.40, 125.15 (q, $^3J_{C-F}$ = 3.9 Hz), 124.23 (q, $^1J_{C-F}$ = 270.6 Hz), 120.72, 115.59 (d, $^2J_{C-F}$ = 21.8 Hz), 115.22, 98.38, 69.42, 62.33, 53.36, 53.05, 52.94. HRMS (m/z) [M+H]⁺ calcd for C₂₉H₂₈F₄N₃O₂: 526.2118, found: 526.2112. Anal. Calcd for

C₂₉H₂₇F₄N₃O₂: C, 66.28; H, 5.18; N, 8.00. Found: C, 66.71; H, 4.74; N, 8.13.

4.1.1.15. 5-(4-((2-Methoxybenzyl)oxy)phenyl)-3-((4-(4-(trifluoromethyl)benzyl)piperazin-1-yl)methyl)isoxazole (6o).

Purified by flash column chromatography (0% → 10% MeOH in DCM). Yield 91.0%; mp 113.2–113.9 °C. IR (ATR) ν : 3132, 2944, 2802, 1615, 1465, 1326, 1249, 1117, 752 cm⁻¹. ¹H NMR (400 MHz, CDCl₃): δ_H 2.50 (br s, 4H, piperazine), 2.57 (br s, 4H, piperazine), 3.56 (s, 2H, -N-CH₂-Ar), 3.63 (s, 2H, -N-CH₂-isoxazole), 3.87 (s, 3H, Ar-OCH₃), 5.16 (s, 2H, -O-CH₂-Ar), 6.42 (s, 1H, isoxazole-H), 6.92 (d, J = 8.0 Hz, 1H, Ar-H), 6.98 (td, J = 8.0 Hz, 0.8 Hz, 1H, Ar-H), 7.05 (d, J = 8.6 Hz, 2H, Ar-H), 7.31 (td, J = 8.0 Hz, 2.0 Hz, 1H, Ar-H), 7.42–7.44 (m, 3H, Ar-H), 7.56 (d, J = 8.0 Hz, 2H, Ar-H), 7.69 (d, J = 8.6 Hz, 2H, Ar-H). ¹³C NMR (100 MHz, DMSO-*d*₆): δ_C 168.90, 161.75, 159.99, 157.00, 143.27, 129.58, 129.35, 129.29, 127.57 (q, $^2J_{C-F}$ = 31.2 Hz), 127.28, 125.02 (q, $^3J_{C-F}$ = 3.8 Hz), 124.35 (q, $^1J_{C-F}$ = 270.5 Hz), 124.16, 120.31, 119.73, 115.27, 110.96, 99.04, 64.82, 61.22, 55.46, 52.49, 52.45. HRMS (m/z) [M+H]⁺ calcd for C₃₀H₃₁F₃N₃O₃: 538.2318, found: 538.2319. Anal. Calcd for C₃₀H₃₀F₃N₃O₃: C, 67.03; H, 5.62; N, 7.82. Found: C, 67.14; H, 5.24; N, 7.98.

4.1.1.16. 5-(4-((3-Methoxybenzyl)oxy)phenyl)-3-((4-(4-(trifluoromethyl)benzyl)piperazin-1-yl)methyl)isoxazole (6p).

Purified by flash column chromatography (0% → 10% MeOH in DCM). Yield 82.0%; mp 100.8–101.1 °C. IR (ATR) ν : 3119, 2944, 2807, 1614, 1455, 1155, 1117, 1010, 776 cm⁻¹. ¹H NMR (400 MHz, CDCl₃): δ_H 2.50 (br s, 4H, piperazine), 2.57 (br s, 4H, piperazine), 3.56 (s, 2H, -N-CH₂-Ar), 3.63 (s, 2H, -N-CH₂-isoxazole), 3.82 (s, 3H, Ar-OCH₃), 5.09 (s, 2H, -O-CH₂-Ar), 6.42 (s, 1H, isoxazole-H), 6.86–6.89 (m, 1H, Ar-H), 6.98–7.04 (m, 4H, Ar-H), 7.31 (t, J = 7.8 Hz, 1H, Ar-H), 7.43 (d, J = 7.8 Hz, 2H, Ar-H), 7.56 (d, J = 7.8 Hz, 2H, Ar-H), 7.70 (d, J = 8.8 Hz, 2H, Ar-H). ¹³C NMR (100 MHz, CDCl₃): δ_C 169.85, 161.76, 160.14, 159.90, 142.45, 138.00, 129.74, 129.33 (q, $^2J_{C-F}$ = 30.7 Hz), 129.18, 127.38, 125.15 (q, $^3J_{C-F}$ = 3.6 Hz), 124.24 (q, $^1J_{C-F}$ = 270.6 Hz), 120.62, 119.58, 115.27, 113.59, 112.94, 98.32, 69.96, 62.35, 55.25, 53.38, 53.07, 52.97. HRMS (m/z) [M+H]⁺ calcd for C₃₀H₃₁F₃N₃O₃: 538.2318, found: 538.2322. Anal. Calcd for C₃₀H₃₀F₃N₃O₃•0.8 EtOAc: C, 65.58; H, 6.03; N, 6.91. Found: C, 65.23; H, 5.65; N, 6.63.

4.1.1.17. 5-(4-((4-Methoxybenzyl)oxy)phenyl)-3-((4-(4-(trifluoromethyl)benzyl)piperazin-1-yl)methyl)isoxazole (6r).

Purified by flash column chromatography (0% → 10% MeOH in DCM). Yield 82.0%; mp 161.9–162.7 °C. IR (ATR) ν : 3044, 2944, 2801, 1613, 1513, 1324, 1242, 1155, 1127, 802 cm⁻¹. ¹H NMR (400 MHz, CDCl₃): δ_H 2.50 (br s, 4H, piperazine), 2.57 (br s, 4H, piperazine), 3.56 (s, 2H, -N-CH₂-Ar), 3.63 (s, 2H, -N-CH₂-isoxazole), 3.82 (s, 3H, Ar-OCH₃), 5.04 (s, 2H, -O-CH₂-Ar), 6.42 (s, 1H, isoxazole-H), 6.93 (d, J = 9.0 Hz, 2H, Ar-H), 7.03 (d, J = 9.0 Hz, 2H, Ar-H), 7.36 (d, J = 9.0 Hz, 2H, Ar-H), 7.43 (d, J = 8.0 Hz, 2H, Ar-H), 7.56 (d, J = 8.0 Hz, 2H, Ar-H), 7.69 (d, J = 9.0 Hz, 2H, Ar-H). ¹³C NMR (100 MHz, CDCl₃): δ_C 169.88, 161.75, 160.26, 159.61, 142.44, 129.31 (q, $^2J_{C-F}$ = 31.0 Hz), 129.25, 129.16, 128.38, 127.34, 125.14 (q, $^3J_{C-F}$ = 3.8 Hz), 124.23 (q, $^1J_{C-F}$ = 270.5 Hz), 120.48, 115.26, 114.08, 98.27, 69.91, 62.34, 55.30, 53.38, 53.06, 52.97. HRMS (m/z) [M+H]⁺ calcd for C₃₀H₃₁F₃N₃O₃: 538.2318, found: 538.2318. Anal. Calcd for C₃₀H₃₀F₃N₃O₃•0.3 CH₂Cl₂: C, 64.62; H, 5.48; N, 7.46. Found: C, 64.57; H, 5.27; N, 7.38.

4.1.1.18. 5-(4-((3,5-Dimethoxybenzyl)oxy)phenyl)-3-((4-(4-(trifluoromethyl)benzyl)piperazin-1-yl)methyl)isoxazole (6s).

Purified by flash column chromatography (0% → 10% MeOH in DCM). Yield 76.0%; mp 111.3–113.8 °C. IR (ATR) ν : 3044, 2936, 2811, 1591, 1457, 1316, 1250, 1114, 1062, 829 cm⁻¹. ¹H NMR (400 MHz, CDCl₃): δ_H 2.50 (br s, 4H, piperazine), 2.57 (br s, 4H, piperazine),

3.56 (s, 2H, -N-CH₂-Ar), 3.63 (s, 2H, -N-CH₂-isoxazole), 3.80 (s, 6H, Ar-OCH₃), 5.05 (s, 2H, -O-CH₂-Ar), 6.41–6.43 (m, 2H, isoxazole-H, Ar-H), 6.58 (d, *J* = 2.4 Hz, 2H, Ar-H), 7.02 (d, *J* = 9.0 Hz, 2H, Ar-H), 7.43 (d, *J* = 7.8 Hz, 2H, Ar-H), 7.56 (d, *J* = 7.8 Hz, 2H, Ar-H), 7.69 (d, *J* = 9.0 Hz, 2H, Ar-H). ¹³C NMR (100 MHz, CDCl₃): δ_C 169.84, 161.75, 161.09, 160.11, 142.44, 138.79, 129.33 (q, ³*J*_{C-F} = 30.7 Hz), 129.18, 127.37, 125.15 (q, ³*J*_{C-F} = 3.9 Hz), 124.25 (q, ¹*J*_{C-F} = 270.0 Hz), 120.63, 115.28, 105.19, 99.94, 98.33, 70.03, 62.34, 55.36, 53.38, 53.07, 52.97. HRMS (m/z) [M+H]⁺ calcd for C₃₁H₃₃F₃N₃O₄: 568.2423, found: 568.2411. Anal. Calcd for C₃₀H₃₀F₃N₃O₃: C, 65.60; H, 5.68; N, 7.40. Found: C, 65.16; H, 5.38; N, 7.14.

4.1.1.19. 3-((4-(4-(Trifluoromethyl)benzyl)piperazin-1-yl)methyl)-5-(4-((3,4,5-trimethoxybenzyl)oxy)phenyl)isoxazole (**6t**). Purified by flash column chromatography (0% → 10% MeOH in DCM). Yield 81.0%; mp 95.9–97.8 °C. IR (ATR) *ν*: 3111, 2940, 2807, 1592, 1463, 1326, 1239, 1116, 1002, 810 cm⁻¹. ¹H NMR (400 MHz, CDCl₃): δ_H 2.50 (br s, 4H, piperazine), 2.57 (br s, 4H, piperazine), 3.56 (s, 2H, -N-CH₂-Ar), 3.64 (s, 2H, -N-CH₂-isoxazole), 3.85 (s, 3H, Ar-OCH₃), 3.88 (s, 6H, Ar-OCH₃), 5.03 (s, 2H, -O-CH₂-Ar), 6.43 (s, 1H, isoxazole-H), 6.66 (s, 2H, Ar-H), 7.04 (d, *J* = 8.8 Hz, 2H, Ar-H), 7.43 (d, *J* = 7.8 Hz, 2H, Ar-H), 7.55 (d, *J* = 7.8 Hz, 2H, Ar-H), 7.71 (d, *J* = 8.8 Hz, 2H, Ar-H). ¹³C NMR (100 MHz, CDCl₃): δ_C 169.78, 161.78, 160.11, 153.51, 142.43, 137.88, 131.91, 129.32 (q, ²*J*_{C-F} = 32.5 Hz), 129.17, 127.40, 125.15 (q, ³*J*_{C-F} = 3.9 Hz), 124.24 (q, ¹*J*_{C-F} = 270.6 Hz), 120.72, 115.24, 104.64, 98.37, 70.40, 62.34, 60.85, 56.15, 53.37, 53.07, 52.97. HRMS (m/z) [M+H]⁺ calcd for C₃₂H₃₅F₃N₃O₅: 598.2529, found: 598.2519. Anal. Calcd for C₃₀H₃₀F₃N₃O₃: C, 64.31; H, 5.73; N, 7.03. Found: C, 64.23; H, 5.38; N, 6.74.

4.1.1.20. 3-((4-(3-((4-(4-(Trifluoromethyl)phenyl)piperazin-1-yl)methyl)isoxazol-5-yl)phenoxy)methyl)benzotrile (**7a**). Purified by flash column chromatography (0% → 10% MeOH in DCM). Yield 89.4%; mp 159.5–160.3 °C. IR (ATR) *ν*: 3136, 2814, 2777, 2232, 1615, 1334, 1251, 1105, 797 cm⁻¹. ¹H NMR (400 MHz, CDCl₃): δ_H 2.69 (t, *J* = 4.8 Hz, 4H, piperazine), 3.31 (t, *J* = 4.8 Hz, 4H, piperazine), 3.70 (s, 2H, -N-CH₂-isoxazole), 5.15 (s, 2H, -O-CH₂-Ar), 6.50 (s, 1H, isoxazole-H), 6.92 (d, *J* = 9.0 Hz, 2H, Ar-H), 7.04 (d, *J* = 8.8 Hz, 2H, Ar-H), 7.47 (d, *J* = 9.0 Hz, 2H, Ar-H), 7.52 (t, *J* = 7.6 Hz, 1H, Ar-H), 7.63–7.69 (m, 2H, Ar-H), 7.72–7.75 (m, 3H, Ar-H). ¹³C NMR (100 MHz, CDCl₃): δ_C 169.84, 161.57, 159.60, 153.18, 138.06, 131.76, 131.44, 130.70, 129.50, 127.55, 126.39 (q, ³*J*_{C-F} = 3.8 Hz), 124.70 (q, ¹*J*_{C-F} = 269.1 Hz), 121.06, 120.61 (q, ²*J*_{C-F} = 32.0 Hz), 118.51, 115.23, 114.59, 112.92, 98.52, 68.74, 53.37, 52.80, 47.90. HRMS (m/z) [M+H]⁺ calcd for C₂₉H₂₆F₃N₄O₂: 519.2008, found: 519.2003. Anal. Calcd for C₂₉H₂₅F₃N₄O₂•0.3 CH₂Cl₂: C, 64.69; H, 4.74; N, 10.30. Found: C, 64.25; H, 4.93; N, 10.28.

4.1.1.21. 3-((4-(3-((4-(5-(Trifluoromethyl)pyridin-2-yl)piperazin-1-yl)methyl)isoxazol-5-yl)phenoxy)methyl)benzotrile (**7b**). Purified by flash column chromatography (0% → 10% MeOH in DCM). Yield 89.0%; mp 156.2–157.3 °C. IR (ATR) *ν*: 3149, 2946, 2808, 2226, 1610, 1515, 1431, 1251, 1109, 787 cm⁻¹. ¹H NMR (400 MHz, CDCl₃): δ_H 2.65 (t, *J* = 4.8 Hz, 4H, piperazine), 3.68 (t, *J* = 4.8 Hz, 4H, piperazine), 3.70 (s, 2H, -N-CH₂-isoxazole), 5.15 (s, 2H, -O-CH₂-Ar), 6.50 (s, 1H, isoxazole-H), 6.63 (d, *J* = 8.8 Hz, 1H, Ar-H), 7.04 (d, *J* = 9.2 Hz, 2H, Ar-H), 7.52 (t, *J* = 7.6 Hz, 1H, Ar-H), 7.60–7.69 (m, 3H, Ar-H), 7.73–7.76 (m, 3H, Ar-H), 8.39 (s, 1H, Ar-H). ¹³C NMR (100 MHz, CDCl₃): δ_C 169.84, 161.56, 160.31, 159.60, 145.72 (q, ³*J*_{C-F} = 4.3 Hz), 138.06, 134.48 (q, ³*J*_{C-F} = 3.1 Hz), 131.77, 131.46, 130.70, 129.51, 127.56, 124.57 (q, ¹*J*_{C-F} = 268.3 Hz), 121.05, 118.53, 115.25 (q, ²*J*_{C-F} = 32.7 Hz), 115.23, 112.91, 105.58, 98.52, 68.74, 53.43, 52.73, 44.59. HRMS (m/z) [M+H]⁺ calcd for C₂₈H₂₅F₃N₅O₂: 520.1960, found: 520.1962. Anal. Calcd for C₂₈H₂₄F₃N₅O₂•0.6 CH₂Cl₂: C, 60.21; H, 4.45; N, 12.28. Found: C, 60.14; H, 4.54; N, 12.37.

4.1.1.22. 3-((4-(3-((4-(4-Fluorophenyl)piperazin-1-yl)methyl)isoxazol-5-yl)phenoxy)methyl)benzotrile (**7c**). Purified by flash column chromatography (0% → 10% MeOH in DCM). Yield 51.3%; mp 141.6–142.0 °C. IR (ATR) *ν*: 3084, 2951, 2810, 2229, 1614, 1514, 1250, 1059, 802 cm⁻¹. ¹H NMR (400 MHz, CDCl₃): δ_H 2.71 (t, *J* = 4.8 Hz, 4H, piperazine), 3.15 (t, *J* = 4.8 Hz, 4H, piperazine), 3.70 (s, 2H, -N-CH₂-isoxazole), 5.15 (s, 2H, -O-CH₂-Ar), 6.50 (s, 1H, isoxazole-H), 6.86–6.89 (m, 2H, Ar-H), 6.96 (t, *J* = 8.8 Hz, 2H, Ar-H), 7.04 (d, *J* = 9.0 Hz, 2H, Ar-H), 7.52 (t, *J* = 7.6 Hz, 1H, Ar-H), 7.64 (d, *J* = 7.6 Hz, 1H, Ar-H), 7.68 (d, *J* = 7.6 Hz, 1H, Ar-H), 7.74 (d, *J* = 9.0 Hz, 2H, Ar-H), 7.76 (s, 1H, Ar-H). ¹³C NMR (100 MHz, CDCl₃): δ_C 169.75, 161.74, 159.56, 157.21 (d, ¹*J*_{C-F} = 235.1 Hz), 147.88 (d, ⁴*J*_{C-F} = 2.3 Hz), 138.07, 131.77, 131.46, 130.70, 129.51, 127.55, 121.11, 118.53, 117.91 (d, ³*J*_{C-F} = 7.6 Hz), 115.52 (d, ²*J*_{C-F} = 22.1 Hz), 115.22, 112.91, 99.55, 68.74, 53.40, 53.14, 50.09. HRMS (m/z) [M+H]⁺ calcd for C₂₈H₂₅FN₄O₂•0.5 EtOAc: C, 70.30; H, 5.70; N, 10.93. Found: C, 70.15; H, 5.35; N, 10.64.

4.1.1.23. 3-((4-(3-((4-(4-Fluorobenzyl)piperazin-1-yl)methyl)isoxazol-5-yl)phenoxy)methyl)benzotrile (**7d**). Purified by flash column chromatography (0% → 10% MeOH in DCM). Yield 76.5%; mp 128.5–129.5 °C. IR (ATR) *ν*: 3110, 2944, 2807, 2235, 1614, 1508, 1428, 1240, 1010, 795 cm⁻¹. ¹H NMR (400 MHz, CDCl₃): δ_H 2.50 (br s, 4H, piperazine), 2.57 (br s, 4H, piperazine), 3.49 (s, 2H, -N-CH₂-Ar), 3.64 (s, 2H, -N-CH₂-isoxazole), 5.14 (s, 2H, -O-CH₂-Ar), 6.45 (s, 1H, isoxazole-H), 6.98 (t, *J* = 8.4 Hz, 2H, Ar-H), 7.02 (d, *J* = 8.6 Hz, 2H, Ar-H), 7.25–7.29 (m, 2H, Ar-H), 7.51 (t, *J* = 7.6 Hz, 1H, Ar-H), 7.64 (d, *J* = 7.6 Hz, 1H, Ar-H), 7.67 (d, *J* = 7.6 Hz, 1H, Ar-H), 7.72 (d, *J* = 8.6 Hz, 2H, Ar-H), 7.75 (s, 1H, Ar-H). ¹³C NMR (100 MHz, CDCl₃): δ_C 169.58, 162.02 (d, ¹*J*_{C-F} = 243.8 Hz), 161.80, 159.51, 138.09, 131.76, 131.45, 130.70, 130.64, (d, ³*J*_{C-F} = 7.0 Hz), 129.49, 127.51, 121.16, 118.52, 115.19, 115.01 (d, ²*J*_{C-F} = 21.4 Hz), 112.91, 98.58, 68.73, 62.08, 53.34, 53.02, 52.79. HRMS (m/z) [M+H]⁺ calcd for C₂₉H₂₈FN₄O₂: 483.2196, found: 483.2183. Anal. Calcd for C₂₉H₂₇FN₄O₂: C, 72.18; H, 5.64; N, 11.61. Found: C, 72.30; H, 5.45; N, 11.67.

4.1.1.24. 3-((4-(3-((4-(2-Fluorobenzyl)piperazin-1-yl)methyl)isoxazol-5-yl)phenoxy)methyl)benzotrile (**7e**). Purified by flash column chromatography (0% → 10% MeOH in DCM). Yield 73.3%; mp 104.6–105.1 °C. IR (ATR) *ν*: 3138, 2955, 2804, 2227, 1612, 1433, 1225, 767 cm⁻¹. ¹H NMR (400 MHz, CDCl₃): δ_H 2.55–2.59 (br s, 8H, piperazine), 3.63 (s, 4H, -N-CH₂-Ar, -N-CH₂-isoxazole), 5.14 (s, 2H, -O-CH₂-Ar), 6.45 (s, 1H, isoxazole-H), 6.99–7.04 (m, 3H, Ar-H), 7.09 (t, *J* = 7.2 Hz, 1H, Ar-H), 7.21–7.25 (m, 1H, Ar-H), 7.37 (t, *J* = 7.2 Hz, 1H, Ar-H), 7.52 (t, *J* = 7.6 Hz, 1H, Ar-H), 7.63 (d, *J* = 7.6 Hz, 1H, Ar-H), 7.67 (d, *J* = 7.6 Hz, 1H, Ar-H), 7.71 (d, *J* = 8.4 Hz, 2H, Ar-H), 7.75 (s, 1H, Ar-H). ¹³C NMR (100 MHz, CDCl₃): δ_C 169.58, 161.82, 161.41 (d, ¹*J*_{C-F} = 244.0 Hz), 159.50, 138.09, 131.75, 131.67 (d, ³*J*_{C-F} = 3.8 Hz), 131.45, 130.70, 129.49, 128.87 (d, ³*J*_{C-F} = 7.6 Hz), 127.51, 123.86 (d, ⁴*J*_{C-F} = 3.8 Hz), 121.16, 118.52, 115.24 (d, ²*J*_{C-F} = 22.1 Hz), 115.18, 112.90, 98.58, 68.72, 55.04, 53.33, 52.99, 52.54. HRMS (m/z) [M+H]⁺ calcd for C₂₉H₂₈FN₄O₂: 483.2196, found: 483.2176. Anal. Calcd for C₂₉H₂₇FN₄O₂•0.2 CH₂Cl₂: C, 70.21; H, 5.53; N, 11.22. Found: C, 70.56; H, 5.42; N, 10.92.

4.1.1.25. 3-((4-(3-((4-(3-Fluorobenzyl)piperazin-1-yl)methyl)isoxazol-5-yl)phenoxy)methyl)benzotrile (**7f**). Purified by flash column chromatography (0% → 10% MeOH in DCM). Yield 55.0%; mp 111.1–112.0 °C. IR (ATR) *ν*: 3115, 2942, 2808, 2233, 1613, 1511, 1428, 1250, 1133, 798 cm⁻¹. ¹H NMR (400 MHz, CDCl₃): δ_H 2.51 (br s, 4H, piperazine), 2.60 (br s, 4H, piperazine), 3.52 (s, 4H, -N-CH₂-Ar), 3.64 (s, 4H, -N-CH₂-isoxazole), 5.14 (s, 2H, -O-CH₂-Ar), 6.46 (s, 1H, isoxazole-H), 6.91–6.96 (m, 1H, Ar-H), 7.01–7.09 (m, 4H, Ar-H), 7.23–7.29 (m, 1H, Ar-H), 7.52 (t, *J* = 7.6 Hz, 1H, Ar-H), 7.64 (d,

$J = 7.6$ Hz, 1H, Ar–H), 7.68 (d, $J = 7.6$ Hz, 1H, Ar–H), 7.73 (d, $J = 8.4$ Hz, 2H, Ar–H), 7.76 (s, 1H, Ar–H). ^{13}C NMR (100 MHz, CDCl_3): δ_{C} 169.60, 162.93 (d, $^1J_{\text{C-F}} = 243.8$ Hz), 161.77, 159.51, 138.10, 131.76, 131.45, 130.70, 129.62 (d, $^3J_{\text{C-F}} = 8.4$ Hz), 129.50, 127.53, 124.54, 121.17, 118.53, 115.75 (d, $^2J_{\text{C-F}} = 21.3$ Hz), 115.20, 113.96 (d, $^2J_{\text{C-F}} = 21.3$ Hz), 112.91, 98.59, 68.73, 62.30, 53.34, 53.03, 52.86. HRMS (m/z) $[\text{M}+\text{H}]^+$ calcd for $\text{C}_{29}\text{H}_{28}\text{FN}_4\text{O}_2$: 483.2196, found: 483.2174.

4.1.1.26. Tert-butyl-4-((3-((4-((3-cyanobenzyl)oxy)phenyl)isoxazol-3-yl)methyl) piperazine-1-carboxylate (7g). Purified by flash column chromatography (0% → 10% MeOH in DCM). Yield 61.3%; mp 132.2–132.6 °C. IR (ATR) ν : 3129, 2972, 2818, 2230, 1682, 1613, 1424, 1242, 1129, 795 cm^{-1} . ^1H NMR (400 MHz, CDCl_3): δ_{H} 1.45 (s, 9H, $-\text{O}-\text{C}(\text{CH}_3)_3$), 2.48 (br t, 4H, piperazine), 3.45 (br t, 4H, piperazine), 3.64 (s, 4H, $-\text{N}-\text{CH}_2$ -isoxazole), 5.14 (s, 2H, $-\text{O}-\text{CH}_2$ -Ar), 6.45 (s, 1H, isoxazole-H), 7.03 (d, $J = 8.8$ Hz, 2H, Ar–H), 7.51 (t, $J = 7.6$ Hz, 1H, Ar–H), 7.63 (d, $J = 7.6$ Hz, 1H, Ar–H), 7.67 (d, $J = 7.6$ Hz, 1H, Ar–H), 7.73 (d, $J = 8.8$ Hz, 2H, Ar–H), 7.75 (s, 1H, Ar–H). ^{13}C NMR (100 MHz, CDCl_3): δ_{C} 169.75, 161.55, 159.55, 154.68, 138.06, 131.76, 131.44, 130.69, 129.49, 127.53, 121.06, 118.51, 115.20, 112.90, 98.49, 79.73, 68.72, 53.43, 52.85, 28.39. HRMS (m/z) $[\text{M}+\text{H}]^+$ calcd for $\text{C}_{27}\text{H}_{31}\text{N}_4\text{O}_4$: 475.2345, found: 475.2334. Anal. Calcd for $\text{C}_{27}\text{H}_{30}\text{N}_4\text{O}_4 \cdot 0.3 \text{CH}_2\text{Cl}_2$: C, 65.57; H, 6.17; N, 11.20. Found: C, 65.80; H, 6.26; N, 11.03.

4.1.1.27. 3-((4-((3-((4-(Furan-2-carbonyl)piperazin-1-yl)methyl)isoxazol-5-yl)phenoxy)methyl) benzonitrile (7h). Purified by flash column chromatography (0% → 10% MeOH in DCM). Yield 68.7%; mp 118.7–119.9 °C. IR (ATR) ν : 3145, 2993, 2823, 2229, 1606, 1435, 1253, 1179, 772 cm^{-1} . ^1H NMR (400 MHz, CDCl_3): δ_{H} 2.60 (t, $J = 5.0$ Hz, 4H, piperazine), 3.67 (s, 2H, $-\text{N}-\text{CH}_2$ -isoxazole), 3.83 (br s, 4H, piperazine), 5.14 (s, 2H, $-\text{O}-\text{CH}_2$ -Ar), 6.46–6.47 (m, 2H, isoxazole-H, Ar–H), 6.98 (dd, $J = 3.6, 0.8$ Hz, 1H, Ar–H), 7.03 (d, $J = 8.8$ Hz, 2H, Ar–H), 7.45–7.46 (m, 1H, Ar–H), 7.51 (t, $J = 7.6$ Hz, 1H, Ar–H), 7.63 (d, $J = 7.6$ Hz, 1H, Ar–H), 7.67 (d, $J = 7.6$ Hz, 1H, Ar–H), 7.73 (d, $J = 8.8$ Hz, 2H, Ar–H), 7.75 (s, 1H, Ar–H). ^{13}C NMR (100 MHz, CDCl_3): δ_{C} 169.86, 161.37, 159.60, 159.06, 147.90, 143.64, 138.06, 131.75, 131.43, 130.69, 129.48, 127.55, 121.03, 118.57, 116.42, 115.23, 112.92, 111.26, 98.45, 68.74, 53.28, 53.20. HRMS (m/z) $[\text{M}+\text{H}]^+$ calcd for $\text{C}_{27}\text{H}_{25}\text{N}_4\text{O}_4$: 469.1876, found: 469.1870.

4.1.1.28. 3-((4-((3-((4-(Tetrahydrofuran-2-carbonyl)piperazin-1-yl)methyl)isoxazol-5-yl)phenoxy) methyl)benzonitrile (7i). Purified by flash column chromatography (0% → 10% MeOH in DCM). Yield 60.1%; mp 109.8–111.2 °C. IR (ATR) ν : 3142, 2936, 2813, 2231, 1656, 1618, 1435, 1242, 1017, 800 cm^{-1} . ^1H NMR (400 MHz, CDCl_3): δ_{H} 1.86–2.04 (m, 3H), 2.24–2.29 (m, 1H), 2.53 (br s, 4H, piperazine), 3.55–3.65 (m, 6H), 3.80–3.95 (m, 2H), 4.58 (t, $J = 6.9$ Hz, tetrahydrofuran CH), 5.14 (s, 2H, $-\text{O}-\text{CH}_2$ -Ar), 6.46 (s, 1H, isoxazole-H), 7.02 (d, $J = 8.6$ Hz, 2H, Ar–H), 7.51 (t, $J = 7.6$ Hz, 1H, Ar–H), 7.63 (d, $J = 7.6$ Hz, 1H, Ar–H), 7.67 (d, $J = 7.6$ Hz, 1H, Ar–H), 7.72 (d, $J = 8.6$ Hz, 2H, Ar–H), 7.75 (s, 1H, Ar–H). ^{13}C NMR (100 MHz, CDCl_3): δ_{C} 169.86, 169.80, 159.59, 138.04, 131.76, 131.44, 130.69, 129.49, 127.55, 121.00, 118.50, 115.22, 112.90, 98.46, 75.84, 69.06, 68.72, 53.27, 53.14, 52.79, 45.21, 41.83, 28.39, 25.70. HRMS (m/z) $[\text{M}+\text{H}]^+$ calcd for $\text{C}_{27}\text{H}_{29}\text{N}_4\text{O}_4$: 473.2189, found: 473.2181.

4.1.1.29. 3-((4-((3-((4-(Tetrahydrofuran-2-yl)methyl)piperazin-1-yl)methyl)isoxazol-5-yl)phenoxy)methyl)benzonitrile (7j). Purified by flash column chromatography (0% → 10% MeOH in DCM). Yield 35.0%; mp 90.8–91.8 °C. IR (ATR) ν : 3120, 2943, 2804, 2228, 1614, 1517, 1442, 1261, 1249, 1059, 836 cm^{-1} . ^1H NMR (400 MHz, CDCl_3): δ_{H} 1.43–1.52 (m, 1H), 1.77–1.90 (m, 2H), 1.92–2.03 (m, 1H), 2.41 (dd, $J = 13.0, 4.0$ Hz, 1H), 2.49 (dd, $J = 13.0, 4.0$ Hz, 1H), 2.58 (s, 8H), 3.62 (s, 2H), 3.69–3.83 (m, 1H), 3.85–3.89 (m, 1H), 3.98–4.05 (m, 1H),

5.13 (s, 2H, $-\text{O}-\text{CH}_2$ -Ar), 6.45 (s, 1H, isoxazole-H), 7.02 (d, $J = 8.8$ Hz, 2H, Ar–H), 7.51 (t, $J = 7.6$ Hz, 1H, Ar–H), 7.63 (d, $J = 7.6$ Hz, 1H, Ar–H), 7.67 (d, $J = 7.6$ Hz, 1H, Ar–H), 7.71 (d, $J = 8.8$ Hz, 2H, Ar–H), 7.75 (s, 1H, Ar–H). ^{13}C NMR (100 MHz, CDCl_3): δ_{C} 169.52, 161.90, 159.47, 138.09, 131.74, 131.45, 130.69, 129.48, 127.50, 121.20, 118.52, 115.17, 112.89, 98.61, 68.72, 68.12, 63.26, 53.63, 53.37, 52.97, 30.36, 25.37. HRMS (m/z) $[\text{M}+\text{H}]^+$ calcd for $\text{C}_{27}\text{H}_{31}\text{N}_4\text{O}_3$: 459.2396, found: 459.2393. Anal. Calcd for $\text{C}_{27}\text{H}_{30}\text{N}_4\text{O}_3 \cdot 0.5 \text{CH}_2\text{Cl}_2$: C, 65.93; H, 6.24; N, 11.18. Found: C, 65.59; H, 6.33; N, 11.63.

4.1.1.30. 3-((4-((3-((4-(Cyclopropanecarbonyl)piperazin-1-yl)methyl)isoxazol-5-yl)phenoxy) methyl)benzonitrile (7k). Purified by flash column chromatography (0% → 10% MeOH in DCM). Yield 66.6%; mp 125.8–126.8 °C. IR (ATR) ν : 3005, 2946, 2849, 2232, 1644, 1609, 1439, 1253, 1230, 1031, 796 cm^{-1} . ^1H NMR (400 MHz, CDCl_3): δ_{H} 0.72–0.77 (m, 2H, cyclopropane CH_2), 0.95–0.99 (m, 2H, cyclopropane CH_2), 1.68–1.74 (m, 1H, cyclopropane CH), 2.55 (br s, 4H, piperazine), 3.65 (s, 2H, $-\text{N}-\text{CH}_2$ -isoxazole), 3.67 (br s, 4H, piperazine), 5.14 (s, 2H, $-\text{O}-\text{CH}_2$ -Ar), 6.46 (s, 1H, isoxazole-H), 7.03 (d, $J = 9.0$ Hz, 2H, Ar–H), 7.51 (t, $J = 7.6$ Hz, 1H, Ar–H), 7.63 (d, $J = 7.6$ Hz, 1H, Ar–H), 7.67 (d, $J = 7.6$ Hz, 1H, Ar–H), 7.73 (d, $J = 9.0$ Hz, 2H, Ar–H), 7.75 (s, 1H, Ar–H). ^{13}C NMR (100 MHz, CDCl_3): δ_{C} 171.95, 169.83, 161.44, 159.59, 138.05, 131.76, 131.44, 130.70, 129.50, 127.55, 121.02, 118.51, 115.22, 112.90, 98.47, 68.73, 53.32, 53.14, 52.84, 45.32, 41.99, 10.89, 7.41. HRMS (m/z) $[\text{M}+\text{H}]^+$ calcd for $\text{C}_{26}\text{H}_{27}\text{N}_4\text{O}_3$: 443.2083, found: 443.2078. Anal. Calcd for $\text{C}_{26}\text{H}_{26}\text{N}_4\text{O}_3 \cdot 0.25 \text{CH}_2\text{Cl}_2$: C, 67.99; H, 5.76; N, 12.08. Found: C, 68.28; H, 5.872; N, 11.68.

4.1.1.31. 3-((4-((3-((4-(Cyclopropylmethyl)piperazin-1-yl)methyl)isoxazol-5-yl)phenoxy) methyl)benzonitrile (7l). Purified by flash column chromatography (0% → 10% MeOH in DCM). Yield 48.0%; mp 98.7–99.3 °C. IR (ATR) ν : 3078, 2945, 2808, 2229, 1616, 1514, 1434, 1253, 1173, 797 cm^{-1} . ^1H NMR (400 MHz, CDCl_3): δ_{H} 0.07–0.11 (m, 2H, cyclopropane CH_2), 0.48–0.51 (m, 2H, cyclopropane CH_2), 0.84–0.87 (m, 1H, cyclopropane CH), 2.26 (d, $J = 6.8$ Hz, 2H, piperazine- CH_2 -cyclopropane), 2.60 (s, 8H, piperazine), 3.64 (s, 4H, $-\text{N}-\text{CH}_2$ -isoxazole), 5.14 (s, 2H, $-\text{O}-\text{CH}_2$ -Ar), 6.45 (s, 1H, isoxazole-H), 7.02 (d, $J = 8.6$ Hz, 2H, Ar–H), 7.51 (t, $J = 7.6$ Hz, 1H, Ar–H), 7.63 (d, $J = 7.6$ Hz, 1H, Ar–H), 7.67 (d, $J = 7.6$ Hz, 1H, Ar–H), 7.72 (d, $J = 8.6$ Hz, 2H, Ar–H), 7.75 (s, 1H, Ar–H). ^{13}C NMR (100 MHz, CDCl_3): δ_{C} 169.54, 161.86, 159.48, 138.09, 131.75, 131.44, 130.69, 129.48, 127.50, 121.19, 118.51, 115.18, 112.90, 98.60, 68.72, 63.68, 53.41, 53.10, 53.05, 8.28, 3.87. HRMS (m/z) $[\text{M}+\text{H}]^+$ calcd for $\text{C}_{26}\text{H}_{29}\text{N}_4\text{O}_2$: 429.2291, found: 429.2289.

4.1.1.32. 3-((4-((3-(((1-Benzylpiperidin-4-yl)amino)methyl)isoxazol-5-yl)phenoxy) methyl)benzonitrile (7m). Purified by flash column chromatography (0% → 10% MeOH in DCM). Yield 44.7%; mp 93.7–94.8 °C. IR (ATR) ν : 3119, 3060, 2938, 2795, 2229, 1615, 1517, 1434, 1253, 1174, 787 cm^{-1} . ^1H NMR (400 MHz, CDCl_3): δ_{H} 1.40–1.50 (m, 2H, piperidine CH_2), 1.88–1.91 (m, 2H, piperidine CH_2), 2.01–2.07 (m, 2H, piperidine CH_2), 2.53–2.56 (m, 1H, piperidine CH), 2.84–2.87 (m, 2H, piperidine CH_2), 3.50 (s, 2H, $-\text{N}-\text{CH}_2$ -Ar), 3.91 (s, 2H, $-\text{N}-\text{CH}_2$ -isoxazole), 5.13 (s, 2H, $-\text{O}-\text{CH}_2$ -Ar), 6.42 (s, 1H, isoxazole-H), 7.02 (d, $J = 8.4$ Hz, 2H, Ar–H), 7.23–7.31 (m, 5H, Ar–H), 7.51 (t, $J = 7.6$ Hz, 1H, Ar–H), 7.63 (d, $J = 7.6$ Hz, 1H, Ar–H), 7.67 (d, $J = 7.6$ Hz, 1H, Ar–H), 7.72 (d, $J = 8.4$ Hz, 2H, Ar–H), 7.75 (s, 1H, Ar–H). ^{13}C NMR (100 MHz, CDCl_3): δ_{C} 169.55, 163.92, 159.50, 138.09, 131.76, 131.44, 130.70, 129.49, 129.15, 128.18, 127.52, 127.00, 121.17, 118.52, 115.18, 112.90, 97.86, 68.72, 62.98, 54.25, 52.17, 42.03, 32.48. HRMS (m/z) $[\text{M}+\text{H}]^+$ calcd for $\text{C}_{30}\text{H}_{31}\text{N}_4\text{O}_2$: 479.2447, found: 479.2451. Anal. Calcd for $\text{C}_{30}\text{H}_{30}\text{N}_4\text{O}_2 \cdot 0.6 \text{MeOH}$: C, 73.83; H, 6.56; N, 11.25. Found: C, 73.81; H, 6.43; N, 10.89.

4.1.1.33. *Tert-butyl-4-(((5-(4-((3-cyanobenzyl)oxy)phenyl)isoxazol-3-yl)methyl)amino) piperidine-1-carboxylate (7n)*. Purified by flash column chromatography (0%→10% MeOH in DCM). Yield 72.2%; mp 145.3–146.3 °C. IR (ATR) ν : 3341, 3151, 2936, 2851, 2233, 1671, 1617, 1426, 1231, 1170, 1020, 798 cm^{-1} . ^1H NMR (400 MHz, CDCl_3): δ_{H} 1.25–1.34 (m, 2H, piperidine CH_2), 1.44 (s, 9H, $-\text{O}-\text{C}(\text{CH}_3)_3$), 1.86–1.89 (m, 2H, piperidine CH_2), 2.68–2.74 (m, 1H, piperidine CH), 2.77–2.83 (m, 2H, piperidine CH_2), 3.93 (m, 2H, piperidine CH_2), 4.01 (br s, 2H, $-\text{N}-\text{CH}_2$ -isoxazole), 5.14 (s, 2H, $-\text{O}-\text{CH}_2$ -Ar), 6.43 (s, 1H, isoxazole-H), 7.02 (d, $J = 8.6$ Hz, 2H, Ar-H), 7.51 (t, $J = 7.6$ Hz, 1H, Ar-H), 7.63 (d, $J = 7.6$ Hz, 1H, Ar-H), 7.67 (d, $J = 7.6$ Hz, 1H, Ar-H), 7.71 (d, $J = 8.6$ Hz, 2H, Ar-H), 7.75 (s, 1H, Ar-H). ^{13}C NMR (100 MHz, CDCl_3): δ_{C} 169.72, 163.52, 159.57, 154.78, 138.07, 131.74, 131.42, 130.68, 129.48, 127.53, 121.09, 118.49, 115.21, 112.92, 97.80, 79.44, 68.74, 54.24, 42.43, 41.90, 32.23, 28.43. HRMS (m/z) $[\text{M}+\text{H}]^+$ calcd for $\text{C}_{28}\text{H}_{33}\text{N}_4\text{O}_4$: 489.2502, found: 489.2508. Anal. Calcd for $\text{C}_{28}\text{H}_{32}\text{N}_4\text{O}_4 \cdot 0.2 \text{CH}_2\text{Cl}_2$: C, 66.56; H, 6.43; N, 10.99. Found: C, 66.37; H, 6.71; N, 10.89.

4.1.1.34. *3-((3-Methyl-4-(3-((4-(4-(trifluoromethyl)benzyl)piperazin-1-yl)methyl)isoxazol-5-yl)phenoxy)methyl)benzotrile (13a)*. Purified by flash column chromatography (0%→10% MeOH in DCM). Yield 32.0%; mp 122.3–123.6 °C. IR (ATR) ν : 3038, 2939, 2817, 2227, 1615, 1320, 1124, 1062, 798 cm^{-1} . ^1H NMR (400 MHz, CDCl_3): δ_{H} 2.49 (s, 3H, Ar- CH_3), 2.58 (br s, 4H, piperazine), 2.66 (br s, 4H, piperazine), 3.61 (s, 2H, $-\text{N}-\text{CH}_2$ -Ar), 3.71 (s, 2H, $-\text{N}-\text{CH}_2$ -isoxazole), 5.12 (s, 2H, $-\text{O}-\text{CH}_2$ -Ar), 6.42 (s, 1H, isoxazole-H), 6.85–6.88 (m, 2H, Ar-H), 7.45–7.52 (m, 3H, Ar-H), 7.57 (d, $J = 8.4$ Hz, 2H, Ar-H), 7.62 (d, $J = 7.6$ Hz, 1H, Ar-H), 7.66 (d, $J = 8.4$ Hz, 2H, Ar-H), 7.74 (s, 1H, Ar-H). ^{13}C NMR (100 MHz, $\text{DMSO}-d_6$): δ_{C} 168.71, 161.28, 159.00, 143.29, 138.49, 137.74, 132.40, 131.70, 131.02, 129.74, 129.68, 129.31, 127.54 (q, $^2J_{\text{C-F}} = 31.6$ Hz), 124.99 (q, $^3J_{\text{C-F}} = 4.1$ Hz), 124.32 (q, $^1J_{\text{C-F}} = 270.4$ Hz), 119.67, 118.62, 117.51, 112.66, 111.45, 102.15, 68.03, 61.21, 52.49, 52.44, 21.22. HRMS (m/z) $[\text{M}+\text{H}]^+$ calcd for $\text{C}_{31}\text{H}_{30}\text{F}_3\text{N}_4\text{O}_2$: 547.2321, found: 547.2325. Anal. Calcd for $\text{C}_{31}\text{H}_{29}\text{F}_3\text{N}_4\text{O}_2$: C, 68.12; H, 5.35; N, 10.25. Found: C, 67.89; H, 5.45; N, 10.16.

4.1.1.35. *3-((2-Methyl-4-(3-((4-(4-(trifluoromethyl)benzyl)piperazin-1-yl)methyl) isoxazol-5-yl)phenoxy)methyl)benzotrile (13b)*. Purified by flash column chromatography (0%→10% MeOH in DCM). Yield 19.0%; mp 124.3–125.0 °C. IR (ATR) ν : 3130, 2937, 2808, 2233, 1617, 1328, 1117, 1055, 806 cm^{-1} . ^1H NMR (400 MHz, CDCl_3): δ_{H} 2.33 (s, 3H, Ar- CH_3), 2.58 (br s, 4H, piperazine), 2.66 (br s, 4H, piperazine), 3.61 (s, 2H, $-\text{N}-\text{CH}_2$ -Ar), 3.69 (s, 2H, $-\text{N}-\text{CH}_2$ -isoxazole), 5.15 (s, 2H, $-\text{O}-\text{CH}_2$ -Ar), 6.50 (s, 1H, isoxazole-H), 6.88 (d, $J = 8.4$ Hz, 1H, Ar-H), 7.46 (d, $J = 8.0$ Hz, 2H, Ar-H), 7.52 (t, $J = 7.6$ Hz, 1H, Ar-H), 7.56–7.59 (m, 4H, Ar-H), 7.64 (d, $J = 7.6$ Hz, 1H, Ar-H), 7.68 (d, $J = 7.6$ Hz, 1H, Ar-H), 7.75 (s, 1H, Ar-H). ^{13}C NMR (75 MHz, $\text{DMSO}-d_6$): δ_{C} 169.46, 162.21, 157.98, 143.72, 139.17, 132.62, 132.15, 131.22, 130.28, 129.82, 128.41, 128.03 (q, $^2J_{\text{C-F}} = 31.5$ Hz), 127.55, 125.48 (q, $^3J_{\text{C-F}} = 3.7$ Hz), 125.24, 124.81 (q, $^1J_{\text{C-F}} = 270.0$ Hz), 120.13, 119.16, 112.55, 111.93, 99.50, 68.60, 61.69, 52.93, 16.50. HRMS (m/z) $[\text{M}+\text{H}]^+$ calcd for $\text{C}_{31}\text{H}_{30}\text{F}_3\text{N}_4\text{O}_2$: 547.2321, found: 547.2330. Anal. Calcd for $\text{C}_{31}\text{H}_{29}\text{F}_3\text{N}_4\text{O}_2$: C, 68.12; H, 5.35; N, 10.25. Found: C, 68.20; H, 5.26; N, 10.61.

4.1.1.36. *3-((3-Fluoro-4-(3-((4-(4-(trifluoromethyl)benzyl)piperazin-1-yl)methyl) isoxazol-5-yl)phenoxy)methyl)benzotrile (13c)*. Purified by flash column chromatography (0%→10% MeOH in DCM). Yield 60.0%; mp 109.7–110.8 °C. IR (ATR) ν : 3044, 2941, 2806, 2234, 1626, 1321, 1166, 1110, 811 cm^{-1} . ^1H NMR (400 MHz, CDCl_3): δ_{H} 2.51 (br s, 4H, piperazine), 2.58 (br s, 4H, piperazine), 3.57 (s, 2H, $-\text{N}-\text{CH}_2$ -Ar), 3.67 (s, 2H, $-\text{N}-\text{CH}_2$ -isoxazole), 5.13 (s, 2H, $-\text{O}-\text{CH}_2$ -Ar), 6.62 (d, $J = 4.0$ Hz, 1H, isoxazole-H), 6.78 (dd, $J = 12.8$ Hz, 2.4 Hz, 1H,

Ar-H), 6.87 (dd, $J = 9.2$ Hz, 2.4 Hz, 1H, Ar-H), 7.44 (d, $J = 8.0$ Hz, 2H, Ar-H), 7.51–7.56 (m, 3H, Ar-H), 7.64–7.67 (m, 2H, Ar-H), 7.74 (s, 1H, Ar-H), 7.87 (t, $J = 8.8$ Hz, 1H, Ar-H). ^{13}C NMR (100 MHz, CDCl_3): δ_{C} 163.66 (d, $^3J_{\text{C-F}} = 3.2$ Hz), 161.84, 160.55 (d, $^3J_{\text{C-F}} = 10.9$ Hz), 160.00 (d, $^1J_{\text{C-F}} = 252.0$ Hz), 137.49, 131.93, 131.44, 130.69, 129.57, 129.22, 128.57 (d, $^3J_{\text{C-F}} = 3.8$ Hz), 125.17 (q, $^3J_{\text{C-F}} = 3.8$ Hz), 124.21 (q, $^1J_{\text{C-F}} = 270.0$ Hz), 118.42, 113.01, 111.21 (d, $^4J_{\text{C-F}} = 3.2$ Hz), 109.57 (d, $^2J_{\text{C-F}} = 12.8$ Hz), 103.14 (d, $^2J_{\text{C-F}} = 25.0$ Hz), 102.39 (d, $^4J_{\text{C-F}} = 10.2$ Hz), 69.07, 62.28, 53.28, 52.90. HRMS (m/z) $[\text{M}+\text{H}]^+$ calcd for $\text{C}_{30}\text{H}_{27}\text{F}_4\text{N}_4\text{O}_2$: 551.2070, found: 551.2073. Anal. Calcd for $\text{C}_{30}\text{H}_{26}\text{F}_4\text{N}_4\text{O}_2$: C, 65.45; H, 4.76; N, 10.18. Found: C, 65.36; H, 4.56; N, 9.84.

4.1.1.37. *3-((2-Fluoro-4-(3-((4-(4-(trifluoromethyl)benzyl)piperazin-1-yl)methyl) isoxazol-5-yl)phenoxy)methyl)benzotrile (13d)*. Purified by flash column chromatography (0%→10% MeOH in DCM). Yield 59.5%; mp 143.2–144.0 °C. IR (ATR) ν : 3075, 2935, 2814, 2228, 1624, 1518, 1323, 1285, 1119, 1064, 789 cm^{-1} . ^1H NMR (400 MHz, CDCl_3): δ_{H} 2.54 (br s, 4H, piperazine), 2.61 (br s, 4H, piperazine), 3.59 (s, 2H, $-\text{N}-\text{CH}_2$ -Ar), 3.66 (s, 2H, $-\text{N}-\text{CH}_2$ -isoxazole), 5.20 (s, 2H, $-\text{O}-\text{CH}_2$ -Ar), 6.50 (s, 1H, isoxazole-H), 7.04 (t, $J = 8.4$ Hz, 1H, Ar-H), 7.44–7.57 (m, 7H, Ar-H), 7.64 (d, $J = 7.6$ Hz, 1H, Ar-H), 7.69 (d, $J = 8.0$ Hz, 1H, Ar-H), 7.76 (s, 1H, Ar-H). ^{13}C NMR (75 MHz, $\text{DMSO}-d_6$): δ_{C} 168.14 (d, $^4J_{\text{C-F}} = 2.2$ Hz), 162.43, 152.18 (d, $^1J_{\text{C-F}} = 243.7$ Hz), 147.84 (d, $^2J_{\text{C-F}} = 10.5$ Hz), 143.71, 138.31, 133.13, 132.48, 131.78, 130.36, 129.82, 128.03 (q, $^2J_{\text{C-F}} = 30.7$ Hz), 125.49 (q, $^3J_{\text{C-F}} = 3.0$ Hz), 124.81 (q, $^1J_{\text{C-F}} = 270.0$ Hz), 122.88 (d, $^4J_{\text{C-F}} = 3.0$ Hz), 120.92 (d, $^3J_{\text{C-F}} = 7.5$ Hz), 119.06, 116.26, 114.05 (d, $^2J_{\text{C-F}} = 20.2$ Hz), 111.99, 100.70, 69.60, 61.68, 52.94, 52.89. HRMS (m/z) $[\text{M}+\text{H}]^+$ calcd for $\text{C}_{30}\text{H}_{27}\text{F}_4\text{N}_4\text{O}_2$: 551.2070, found: 551.2066. Anal. Calcd for $\text{C}_{30}\text{H}_{26}\text{F}_4\text{N}_4\text{O}_2$: C, 65.45; H, 4.76; N, 10.18. Found: C, 65.36; H, 4.57; N, 9.79.

4.1.1.38. *3-((2-Fluoro-4-(3-((4-(4-(furan-2-carbonyl)piperazin-1-yl)methyl)isoxazol-5-yl)phenoxy)methyl)benzotrile (14)*. Purified by flash column chromatography (0%→10% MeOH in DCM). Yield 83.0%; mp 129.9–131.2 °C. IR (ATR) ν : 3111, 2941, 2804, 2231, 1604, 1519, 1442, 1285, 1118, 802 cm^{-1} . ^1H NMR (400 MHz, CDCl_3): δ_{H} 2.61 (br s, 4H, piperazine), 3.69 (s, 2H, $-\text{N}-\text{CH}_2$ -isoxazole), 3.84 (br s, 4H, piperazine), 5.21 (s, 2H, $-\text{O}-\text{CH}_2$ -Ar), 6.47 (dd, $J = 3.6, 2.0$ Hz, 1H), 6.51 (s, 1H, isoxazole-H), 6.99 (dd, $J = 3.6, 0.8$ Hz, 1H, Ar-H), 7.05 (t, $J = 8.4$ Hz, 1H, Ar-H), 7.46 (dd, $J = 2.0, 0.8$ Hz, 1H, Ar-H), 7.49–7.55 (m, 3H, Ar-H), 7.65 (d, $J = 7.6$ Hz, 1H, Ar-H), 7.70 (d, $J = 8.0$ Hz, 1H, Ar-H), 7.76 (s, 1H, Ar-H). ^{13}C NMR (100 MHz, CDCl_3): δ_{C} 168.65 (d, $^4J_{\text{C-F}} = 2.6$ Hz), 161.60, 159.01, 152.72 (d, $^1J_{\text{C-F}} = 246.8$ Hz), 147.87, 147.68 (d, $^2J_{\text{C-F}} = 10.3$ Hz), 143.67, 137.55, 131.96, 131.50, 130.70, 129.59, 122.22 (d, $^4J_{\text{C-F}} = 3.9$ Hz), 121.61 (d, $^3J_{\text{C-F}} = 7.7$ Hz), 118.45, 116.47, 115.66 (d, $^4J_{\text{C-F}} = 2.0$ Hz), 114.20 (d, $^2J_{\text{C-F}} = 20.5$ Hz), 112.96, 111.28, 99.28, 70.04, 53.23, 53.10. HRMS (m/z) $[\text{M}+\text{H}]^+$ calcd for $\text{C}_{27}\text{H}_{24}\text{FN}_4\text{O}_4$: 487.1782, found: 487.1781. Anal. Calcd for $\text{C}_{27}\text{H}_{23}\text{FN}_4\text{O}_4$: C, 66.66; H, 4.77; N, 11.52. Found: C, 66.72; H, 4.83; N, 11.62.

4.1.1.39. *3-((4-(3-(((1-Benzylpiperidin-4-yl)amino)methyl)isoxazol-5-yl)-2-fluorophenoxy)methyl)benzotrile (15)*. Purified by flash column chromatography (0%→10% MeOH in DCM). Yield 68.5%; mp 78.1–79.5 °C. IR (ATR) ν : 3323, 3146, 2940, 2808, 2234, 1622, 1435, 1283, 1131, 1096, 810 cm^{-1} . ^1H NMR (400 MHz, CDCl_3): δ_{H} 1.47–1.51 (m, 2H, piperidine CH_2), 1.91–1.93 (m, 2H, piperidine CH_2), 2.09 (br s, 2H, piperidine CH_2), 2.57 (br s, 1H, piperidine CH), 2.87–2.91 (m, 2H, piperidine CH_2), 3.55 (s, 2H, $-\text{N}-\text{CH}_2$ -Ar), 3.91 (s, 2H, $-\text{N}-\text{CH}_2$ -isoxazole), 5.20 (s, 2H, $-\text{O}-\text{CH}_2$ -Ar), 6.44 (s, 1H, isoxazole-H), 7.04 (t, $J = 8.4$ Hz, 1H, Ar-H), 7.26–7.32 (m, 5H, Ar-H), 7.47–7.54 (m, 3H, Ar-H), 7.64 (d, $J = 7.0$ Hz, 1H, Ar-H), 7.70 (d, $J = 7.6$ Hz, 1H, Ar-H), 7.76 (s, 1H, Ar-H). ^{13}C NMR (100 MHz,

CDCl₃: δ_C 168.35, 164.14, 152.72 (d, $^1J_{C-F}$ = 246.2 Hz), 147.59 (d, $^3J_{C-F}$ = 10.9 Hz), 138.53, 137.60, 131.96, 130.71, 131.50, 129.59, 129.09, 128.16, 126.93, 122.18 (d, $^4J_{C-F}$ = 3.2 Hz), 121.81 (d, $^3J_{C-F}$ = 7.1 Hz), 118.46, 115.65 (d, $^4J_{C-F}$ = 1.9 Hz), 114.18 (d, $^2J_{C-F}$ = 20.5 Hz), 112.97, 98.74, 70.06, 63.06, 54.41, 52.26, 42.01, 32.63. HRMS (m/z) [M+H]⁺ calcd for C₃₀H₃₀FN₄O₂: 497.2353, found: 497.2352. Anal. Calcd for C₃₀H₂₉FN₄O₂: C, 72.56; H, 5.89; N, 11.28. Found: C, 73.00; H, 5.60; N, 11.57.

4.2. Biological studies

4.2.1. Cell Culture

Mahlavu (mesenchymal), Huh7, and HepG2 (epithelial) human hepatocellular carcinoma (HCC) cells and MCF-7 (epithelial) human breast cancer carcinoma cells were maintained in Dulbecco's Modified Eagles Medium (DMEM) supplemented with 10% fetal bovine serum (FBS) (Gibco/Thermo Fisher Scientific) and 0.1 mM non-essential amino acid (Gibco/Thermo Fisher Scientific), while SNU-475 cells were cultured in RPMI (Gibco/Thermo Fisher Scientific) supplemented with 10% fetal bovine serum (FBS) (Gibco/Thermo Fisher Scientific) and 2 mM L-Glutamine (Gibco/Thermo Fisher Scientific). Growth mediums contained 100 Units/mL Penicillin/Streptomycin. Cells were maintained in 37 °C in a humidified incubator under %5 CO₂.

4.2.2. NCI-60 sulforhodamine B (SRB) cytotoxicity assay

Mahlavu, SNU-475, Huh7, HepG2 and MCF-7 cells were inoculated in 96-well plates and were grown in an incubator for 24 h. The cells were treated with compound **6a**, compound **13d**, and DMSO (Sigma) control in a concentration range starting from 40 μ M to 0.6 μ M. After 72 h of treatment, the cells were fixed with cold 10% (w/v) trichloroacetic acid (MERCK) for an hour, washed with ddH₂O, and left for drying. The proteins were stained by incubating the plates with sulforhodamine B (SRB) dye solution (Sigma) (50 μ l of a 0.4% (w/v) of SRB in 1% acetic acid (Sigma)) at RT for 10 min. To get rid of unbound SRB dye, the plates were washed with 1% acetic acid for three times and left to air-drying. The protein-bound SRB dye was solubilized using 100 μ l/well 10 mM Tris-Base solution, and their absorbances were measured with 96-well plate reader at 515 nm wavelength (ELx800, BioTek). To check the reproducibility of the data, all experiments were performed in triplicates and DMSO was used as a control for treatment. IC₅₀ values were calculated and only data with R² values larger than 0.9 are considered as significant.

4.2.3. Real-time cell growth surveillance by electronic sensing (RT-CES)

To monitor the cell growth of cells and cytotoxicity of compound **6a** and compound **13d**, the real-time cell growth system (xCelligence, Roche Applied Sciences) was used. The cells were plated onto 96-well E-plate (Mahlavu and SNU-475: 1000 cell/well, Huh7:2500 cell/well, HepG2:3500 cell/well) in 100 μ l of the medium/well. To check the proliferation of the cells, the cellular growth was measured as cell index (CI) every 30 min for 24 h. After treatment with the compounds in 2.5, 5 and 10 μ M concentrations, the CI values were recorded every 10 min for 24 h (fast drug response) and then every 30 min for the remaining time (long-term drug response). The inhibitory effects of compound **6a** and **13d** in response to DMSO controls were analyzed by calculating CI_{compound}/CI_{DMSO}. To check the reproducibility of the data, all experiments were performed in triplicates [34]. Quantitative analysis of RT-CES results for compounds' cytotoxicity doses were also summarized in Table S1. If the IC₅₀ value is larger than 10 μ M or less than 2.5 μ M, it is shown as >10 or <2.5 in table, respectively.

4.2.4. Cell cycle analysis with flow cytometry

Mahlavu, SNU-475, Huh7, and HepG2 cells were cultured onto 100 mm dishes. After 24 h, cells were treated with 5 μ M compound **6a**, compound **13d** and, DMSO as a negative control. At the end of the 48 h and 72 h treatment period, cells were fixed with ice-cold 70% (v/v) EtOH for 3 h at -20 °C. Cell cycle analysis was carried out by PI (Propidium Iodide) staining using flow cytometry according to the Muse™ cell cycle kit manufacturer's recommendations (Millipore, MCH1000106). Analysis of cells were done using Novocyte Flow Cytometer (ACEA).

4.2.5. Cell death analysis with flow cytometry

Mahlavu, SNU-475, Huh7, and HepG2 cells were cultured onto 100 mm dishes. After 24 h, cells were treated with 5 μ M compound **6a** and compound **13d** by keeping DMSO as a negative control. At the end of the 48 h and 72 h treatment period, cells were also collected for programmed cell death Annexin V assay to be stained with PI and Annexin V (Roche, #11 858 777 001) dyes and incubated for 15 min at room temperature in dark prior to analysis by flow cytometry.

4.2.6. Immunofluorescence staining for detection of cell death

Mahlavu and SNU-475 (30.000 cell/well), Huh7 (60.000 cell/well), and HepG2 (100.000 cell/well), cells were seeded onto cover slides for 24 h. Cells were treated with compound **6a**, compound **13d** or DMSO as a control for 24 h, 48 h, and 72 h. Then, cells were washed with 1X PBS three times and fixed with 100% ice-cold methanol to be stained with 1 μ g/ml Hoechst (#33258, Sigma). Nuclei of cells were imaged under fluorescent microscopy for nuclear fragmentation.

4.2.7. Western blotting

Cells were treated for 72 h with 5 μ M of compound **6a** and compound **13d** or DMSO as a control. Cells were collected with a scraper and total lysates were prepared. Protein concentrations were calculated with Bradford assay. The levels of proteins were examined by using protein electrophoresis according to the manufacturer's protocol for Western blot analysis (Mini-PROTEAN® Tetra Cell Systems, Bio-Rad). The compound treated samples were loaded onto TGX™ precast gels (20–40 μ g/well) and proteins were transferred to an LF-PVDF membrane using the Trans-Blot Turbo Transfer System (Bio-Rad) Primary antibodies; phospho-Akt (Ser473) (CST, #9271L), Akt (CST, #9272), Erk 1/2 (CST, #9107S), phospho-Erk 1/2 (Thr202/Tyr204) (CST, 9106S), p53 (Millipore, #05–224), phospho-p53 (Ser15) (CST, #9286S), acetyl-p53 (Lys382) (CST, #2525S), p21/Waf1, Cip1 (CST, #2946), c-Myc (Santa Cruz, #sc42), Calnexin (CST, #2679) and secondary antibodies (IRDye 680RD Goat Anti Mouse (Li-cor, # 92668070), IRDye-800CW Goat Anti Rabbit (Licor, # 926–32211)) were used for immunoblotting, and the proteins were visualized fluorescently using Odyssey CLx- LICOR imaging system [76].

4.2.8. Flow cytometry analysis for detection of cancer cell stemness markers

Mahlavu (100.000 cells/plate) and Huh7 (200.000 cells/plate) cells were cultured into 100 mm² culture plates. After 24 h incubation, cells were treated with 10 μ M Sorafenib, FDA-approved drug for HCC, DAPT (Notch inhibitor) as a positive control, compound **6a**, compound **13d** or DMSO as a negative control for 72 h incubation. All staining procedures and analysis of cells were performed as previously described [9]. Briefly, the plates were washed with 1X PBS to remove dead cells and remained attached cells were collected into tubes to be fixed with 4% paraformaldehyde for 25 min at RT. For anti-CD133 and EpCAM staining in Huh7 cells, cells were washed with FACS buffer and stained using PE anti-

human CD133 (Biolegend, #372804), FITC anti-human CD326 (EpCAM) (Immunostep, #326F-100T) and with their isotype controls PE-Mouse-IgG1 Isotype Control (Immunostep, #ICIGG1PE-50) and FITC-Mouse-IgG1 Isotype Control (Immunostep, #ICIGG1F-100). The similar staining protocol was performed for analysis of HCC cells to detect OCT4 (Alexa Fluor® 488 Mouse anti-Oct3/4, BD Pharmingen, #560253) and NANOG (Alexa Fluor® 647 Mouse anti-Mouse NANOG, BD Pharmingen, #560279) and cancer stemness markers. The 90% (v/v) ice-cold methanol was used to incubate cells before antibody blocking for the detection of stemness marker expressions permeabilization of cells. The stained cells were incubated for 40 min at RT in dark. After staining, the cells were washed with FACS buffer and analyzed using the Novocyte flow cytometer (ACEA Biosciences).

4.2.9. Sphere formation assay

Sphere formation assay was performed as previously described [9]. Briefly, Huh7 (200.000 cells/plate) cells were inoculated into 100 mm² culture plates. After 24 h, cells were treated with 10 µM Sorafenib, DAPT, compound **6a**, compound **13d**, and DMSO for 72h. The plates were washed with 1X PBS to remove non-attached dead cells. The collected cells were inoculated into ultra-low attachment 96-well plates using sphere formation medium for 14 days. Spheres were imaged under light microscopy and sphere size and count measurements were done using the ZEN Blue microscopy software.

4.2.10. Quantitative RT-PCR (qRT-PCR)

After total RNA isolation using the RNeasy RNA-purification kit (Qiagen), cDNA synthesis was performed using the RevertAid First Strand cDNA synthesis kit (Thermo Scientific). The specific stemness markers' and GAPDH as an internal control gene primer sequences used for qRT-PCR are; OCT4 forward primer: 5' CGGAGGAGTCCCAGGACATCAA 3', OCT4 reverse primer: 5' AAATAGAACCCCGGGTGTGAGC 3', NANOG forward primer: 5' TACCTCAGCCTCCAGCAGATG 3', NANOG reverse primer: 5' TCTTCGGCCAGTTGTTTTTCTG 3', and GAPDH forward primer: 5' TATGACAACGAATTTGGCTAC 3', GAPDH reverse primer: 5' TCTCTCTCTCTGTGCTCT 3' and detailed information was shown in Table S3. Quantitative PCR was done using Light Cycler® 480 SYBR Green I Master (Roche) following steps: preincubation at 95 °C for 10 min, amplification for 45 cycles (95 °C 10 s followed by 60 °C 10 s and 72 °C 10 s) and melting at 95 °C 10 s followed by 65 °C for 60 s and 97 °C for 1 s (Table S4). The experimental cycle threshold (Ct) was adjusted against GAPDH control product. All amplifications were performed in triplicates. The $\Delta\Delta C_t$ method was exhibited to determine the amount of target gene in compound treated cells relative to that expressed by control (DMSO) treated cells.

4.3. Statistical analysis

In this study, all data were accessed from three independent experiments and standard deviation (S.D) values were determined accordingly. Student's t-tests were applied using Graphpad (Prism) for statistical analysis. The mean of the fluorescence intensity was used for flow cytometry analysis of cancer stemness markers and results were provided in Figure S1. All experiments were performed with $n \geq 3$ biological replicates. Statistically significant results were shown as follows: ns: not significant, * $p < 0.05$, ** $p < 0.01$, *** $p < 0.001$ and **** $p < 0.0001$.

Declaration of competing interest

The authors declare that they have no known competing financial interests or personal relationships that could have

appeared to influence the work reported in this paper.

Acknowledgements

This study was supported by The Scientific and Technological Research Council of Turkey (TUBITAK Project No. 214S062).

Appendix A. Supplementary data

Supplementary data to this article can be found online at <https://doi.org/10.1016/j.ejmech.2021.113489>.

References

- [1] D. Hanahan, R.A. Weinberg, Hallmarks of cancer: the next generation, *Cell* 144 (2011) 646–674.
- [2] T.A. Wallace, D.N. Martin, S. Ambs, Interactions among genes, tumor biology and the environment in cancer health disparities: examining the evidence on a national and global scale, *Carcinogenesis* 32 (2011) 1107–1121.
- [3] G. Baffy, E.M. Brunt, S.H. Caldwell, Hepatocellular carcinoma in non-alcoholic fatty liver disease: an emerging menace, *J. Hepatol.* 56 (2012) 1384–1391.
- [4] B.W. Stewart, C.P. Wild, *World Cancer Report*, Lyon, 2014.
- [5] B. Sun, M. Karin, Obesity, inflammation, and liver cancer, *J. Hepatol.* 56 (2012) 704–713.
- [6] H. Unsal, C. Yalciner, C. Marçais, M. Kew, M. Volkman, H. Zentgraf, K.J. Isselbacher, M. Ozturk, Genetic heterogeneity of hepatocellular carcinoma, *Proc. Natl. Acad. Sci. U. S. A.* 91 (1994) 822–826.
- [7] E.M.F. De Sousa, L. Vermeulen, E. Fessler, J.P. Medema, Cancer heterogeneity—a multifaceted view, *EMBO Rep.* 14 (2013) 686–695.
- [8] A.K. Chow, L. Ng, C.S. Lam, S.K. Wong, T.M. Wan, N.S. Cheng, T.C. Yau, R.T. Poon, R.W. Pang, The Enhanced metastatic potential of hepatocellular carcinoma (HCC) cells with sorafenib resistance, *PLoS One* 8 (2013), e78675.
- [9] D.C. Kahraman, G. Hanquet, L. Jeanmart, S. Lanners, P. Sramel, A. Bohac, R. Cetin-Atalay, Quinoides and VEGFR2 TKIs influence the fate of hepatocellular carcinoma and its cancer stem cells, *MedChemComm* 8 (2017) 81–87.
- [10] H.W. Xin, C.M. Ambe, D.M. Hari, G.W. Wiegand, T.C. Miller, J.Q. Chen, A.J. Anderson, S. Ray, J.E. Mullinax, T. Koizumi, R.C. Langan, D. Burka, M.A. Herrmann, P.K. Goldsmith, A. Stojadinovic, U. Rudloff, S.S. Thorgeirsson, I. Avital, Label-retaining liver cancer cells are relatively resistant to sorafenib, *Gut* 62 (2013) 1777–1786.
- [11] S. Hoelder, P.A. Clarke, P. Workman, Discovery of small molecule cancer drugs: successes, challenges and opportunities, *Mol. Oncol.* 6 (2012) 155–176.
- [12] V. Lavanya, A.A. Mohammed Adil, A. Neesar, A.K. Rishi, J. Shazia, Small molecule inhibitors as emerging cancer therapeutics, *Integr. Cancer Sci. Therap.* 1 (2014) 39–46.
- [13] A. Sysak, B. Obminska-Mrukowicz, Isoxazole ring as a useful scaffold in a search for new therapeutic agents, *Eur. J. Med. Chem.* 137 (2017) 292–309.
- [14] S.A. Eccles, A. Massey, F.I. Raynaud, S.Y. Sharp, G. Box, M. Valenti, L. Patterson, A. de Haven Brandon, S. Gowan, F. Boxall, W. Aherne, M. Rowlands, A. Hayes, V. Martins, F. Urban, K. Boxall, C. Prodromou, L. Pearl, K. James, T.P. Matthews, K.M. Cheung, A. Kalusa, M. Jones, E. McDonald, X. Barril, P.A. Brough, J.E. Chesfield, B. Dymock, M.J. Drysdale, H. Finch, R. Howes, R.E. Hubbard, A. Surgeon, P. Webb, M. Wood, L. Wright, P. Workman, NVP-AUY922: a novel heat shock protein 90 inhibitor active against xenograft tumor growth, angiogenesis, and metastasis, *Canc. Res.* 68 (2008) 2850–2860.
- [15] E. Felip, F. Barlesi, B. Besse, Q. Chu, L. Gandhi, S.W. Kim, E. Carcereny, L.V. Sequist, P. Brunsvig, C. Chouaid, E.F. Smit, H.J.M. Groen, D.W. Kim, K. Park, E. Avsar, S. Szpakowski, M. Akimov, E.B. Garon, Brief report: phase 2 study of the HSP-90 inhibitor AUY922 in previously treated and molecularly defined patients with advanced non-small cell lung cancer, *J. Thorac. Oncol.* 13 (4) (2017) 576–584.
- [16] C. Zhang, M. Chu, Leflunomide: a promising drug with good antitumor potential, *Biochem. Biophys. Res. Commun.* 496 (2) (2018) 726–730.
- [17] P. Bamborough, H. Diallo, J.D. Goodacre, L. Gordon, A. Lewis, J.T. Seal, D.M. Wilson, M.D. Woodrow, C.W. Chung, Fragment-based discovery of bromodomain inhibitors part 2: optimization of phenylisoxazole sulfonamides, *J. Med. Chem.* 55 (2012) 587–596.
- [18] C.W. Chung, A.W. Dean, J.M. Woolven, P. Bamborough, Fragment-based discovery of bromodomain inhibitors part 1: inhibitor binding modes and implications for lead discovery, *J. Med. Chem.* 55 (2012) 576–586.
- [19] D.S. Hewings, O. Fedorov, P. Filippakopoulos, S. Martin, S. Picaud, A. Tumber, C. Wells, M.M. Olcina, K. Freeman, A. Gill, A.J. Ritchie, D.W. Sheppard, A.J. Russell, E.M. Hammond, S. Knapp, P.E. Brennan, S.J. Conway, Optimization of 3,5-dimethylisoxazole derivatives as potent bromodomain ligands, *J. Med. Chem.* 56 (2013) 3217–3227.
- [20] D.S. Hewings, M. Wang, M. Philpott, O. Fedorov, S. Uttarkar, P. Filippakopoulos, S. Picaud, C. Vuppasetty, B. Marsden, S. Knapp, S.J. Conway, T.D. Heightman, 3,5-dimethylisoxazoles act as acetyl-lysine-mimetic bromodomain ligands, *J. Med. Chem.* 54 (2011) 6761–6770.
- [21] M.K. Akkoc, M.Y. Yuksel, I. Durmaz, R.C. Atalay, Design, synthesis, and

- biological evaluation of indole-based 1,4-disubstituted piperazines as cytotoxic agents, *Turk. J. Chem.* 36 (2012) 515–525.
- [22] Z.W. Mao, X. Zheng, Y. Qi, M.D. Zhang, Y. Huang, C.P. Wan, G.X. Rao, Synthesis and biological evaluation of novel hybrid compounds between chalcone and piperazine as potential antitumor agents, *RSC Adv.* 6 (2016) 7723–7727.
- [23] A.M. Saab, M. Dobmeier, B. Koenig, E. Fabri, A. Finotti, M. Borgatti, I. Lampronti, F. Bernardi, T. Efferth, R. Gambari, Antiproliferative and erythroid differentiation of piperazine and triphenyl derivatives against k-562 human chronic myelogenous leukemia, *Anticancer Res.* 33 (2013) 3027–3032.
- [24] M. Tuncbilek, E.B. Guven, T. Onder, R. Cetin Atalay, Synthesis of novel 6-(4-substituted piperazine-1-yl)-9-(beta-D-ribofuranosyl)purine derivatives, which lead to senescence-induced cell death in liver cancer cells, *J. Med. Chem.* 55 (2012) 3058–3065.
- [25] A.M. Waszkielewicz, A. Gunia, N. Szkaradek, K. Pytka, A. Siwek, G. Satala, A.J. Bojarski, E. Szneler, H. Marona, Synthesis and evaluation of pharmacological properties of some new xanthone derivatives with piperazine moiety, *Bioorg. Med. Chem. Lett.* 23 (2013) 4419–4423.
- [26] Y. Hori, K. Ishii, H. Kanda, Y. Iwamoto, K. Nishikawa, N. Soga, H. Kise, K. Arima, Y. Sugimura, Naftopidil, a selective α 1-adrenoceptor antagonist, suppresses human prostate tumor growth by altering interactions between tumor cells and stroma, *Cancer Prev. Res.* 4 (2011) 87–96.
- [27] H. Kanda, K. Ishii, Y. Ogura, T. Imamura, M. Kanai, K. Arima, Y. Sugimura, Naftopidil, a selective α -1 adrenoceptor antagonist, inhibits growth of human prostate cancer cells by G1 cell cycle arrest, *Int. J. Cancer* 122 (2008) 444–451.
- [28] H. Chen, X. Liang, F. Xu, B. Xu, X. He, B. Huang, M. Yuan, Synthesis and cytotoxic activity evaluation of novel arylpiperazine derivatives on human prostate cancer cell lines, *Molecules* 19 (2014) 12048–12064.
- [29] H. Chen, B.B. Xu, T. Sun, Z. Zhou, H.Y. Ya, M. Yuan, Synthesis and antitumor activity of novel arylpiperazine derivatives containing the saccharin moiety, *Molecules* 22 (2017).
- [30] H. Chen, F. Xu, X. Liang, B.B. Xu, Z.L. Yang, X.L. He, B.Y. Huang, M. Yuan, Design, synthesis and biological evaluation of novel arylpiperazine derivatives on human prostate cancer cell lines, *Bioorg. Med. Chem. Lett.* 25 (2015) 285–287.
- [31] E.H. Cho, S.G. Chung, S.H. Lee, H.S. Kwon, J.E. Lee, D.W. Kang, J.H. Joo, Y.H. Lee, Piperazine Derivatives and Process for the Preparation Thereof, in: *WO1998000402 A1*, 1998.
- [32] J.H. Lee, D.W. Kang, H.S. Kwon, S.H. Lee, S.K. Park, S.G. Chung, E.H. Cho, S.Y. Paik, J.H. Lee, Microtubule inhibitory effects of various Sj compounds on tissue culture cells, *Arch Pharm. Res. (Seoul)* 27 (2004) 436–441.
- [33] A.K. Rathi, R. Syed, H.S. Shin, R.V. Patel, Piperazine derivatives for therapeutic use: a patent review (2010-present), *Expert Opin. Ther. Pat.* 26 (2016) 777–797.
- [34] B. Caliskan, E. Sinoplu, K. İbiş, E. Akhan Guzelcan, R. Cetin Atalay, E. Banoglu, Synthesis and cellular bioactivities of novel isoxazole derivatives incorporating an arylpiperazine moiety as anticancer agents, *J. Enzym. Inhib. Med. Chem.* 33 (2018) 1352–1361.
- [35] O. Akbulut, D. Lengerli, O. Saatici, E. Duman, U.O.S. Seker, A. Isik, A. Akyol, B. Caliskan, E. Banoglu, O. Sahin, A highly potent TACC3 inhibitor as a novel anticancer drug candidate, *Mol. Canc. Therapeut.* 19 (2020) 1243–1254.
- [36] S.N. Baytas, N. Incelcer, A. Yilmaz, A. Olgac, S. Menevse, E. Banoglu, E. Hamel, R. Bortolozzi, G. Viola, Synthesis, biological evaluation and molecular docking studies of trans-indole-3-acrylamide derivatives, a new class of tubulin polymerization inhibitors, *Bioorg. Med. Chem.* 22 (2014) 3096–3104.
- [37] B. Caliskan, A. Yilmaz, I. Evren, S. Menevse, O. Uludag, E. Banoglu, Synthesis and evaluation of analgesic, anti-inflammatory, and anticancer activities of new pyrazole-3(5)-carboxylic acid derivatives, *Med. Chem. Res.* 22 (2013) 782–793.
- [38] S. Cankara Pırol, B. Caliskan, I. Durmaz, R. Atalay, E. Banoglu, Synthesis and preliminary mechanistic evaluation of 5-(p-tolyl)-1-(quinolin-2-yl)pyrazole-3-carboxylic acid amides with potent antiproliferative activity on human cancer cell lines, *Eur. J. Med. Chem.* 87 (2014) 140–149.
- [39] P. Skehan, R. Storeng, D. Scudiero, A. Monks, J. McMahon, D. Vistica, J.T. Warren, H. Bokesch, S. Kenney, M.R. Boyd, New colorimetric cytotoxicity assay for anticancer-drug screening, *J. Natl. Cancer Inst.* 82 (1990) 1107–1112.
- [40] K. Solly, X. Wang, X. Xu, B. Strulovici, W. Zheng, Application of real-time cell electronic sensing (RT-CES) technology to cell-based assays, *Assay Drug Dev. Technol.* 2 (2004) 363–372.
- [41] J. Chen, The cell-cycle arrest and apoptotic functions of p53 in tumor initiation and progression, *Cold Spring Harb Perspect Med* 6 (2016) a026104.
- [42] W.S. el-Deiry, T. Tokino, V.E. Velculescu, D.B. Levy, R. Parsons, J.M. Trent, D. Lin, W.E. Mercer, K.W. Kinzler, B. Vogelstein, WAF1, a potential mediator of p53 tumor suppression, *Cell* 75 (1993) 817–825.
- [43] J.W. Harper, G.R. Adami, N. Wei, K. Keyomarsi, S.J. Elledge, The p21 Cdk-interacting protein Cip1 is a potent inhibitor of G1 cyclin-dependent kinases, *Cell* 75 (1993) 805–816.
- [44] V.S. Romanov, K.L. Rudolph, p21 shapes cancer evolution, *Nat. Cell Biol.* 18 (2016) 722–724.
- [45] B. Bhardwaj, G. Bhardwaj, J.Y. Lau, Expression of p21 and p27 in hepatoma cell lines with different p53 gene profile, *J. Hepatol.* 31 (1999) 386.
- [46] M.S. Kang, H.J. Lee, J.H. Lee, J.L. Ku, K.P. Lee, M.J. Kelley, Y.J. Won, S.T. Kim, J.G. Park, Mutation of p53 gene in hepatocellular carcinoma cell lines with HBX DNA, *Int. J. Cancer* 67 (1996) 898–902.
- [47] A.A. Elbendary, F.D. Cirisano, A.C. Evans, P.L. Davis, J.D. Iglehart, J.R. Marks, A. Berchuck, Relationship between p21 expression and mutation of the p53 tumor suppressor gene in normal and malignant ovarian epithelial cells, *Clin. Canc. Res.* 2 (9) (1996) 1571–1575.
- [48] H. Zhao, F. Traganos, Z. Darzynkiewicz, Phosphorylation of p53 on Ser15 during cell cycle caused by Topo I and Topo II inhibitors in relation to ATM and Chk2 activation, *Cell Cycle* 7 (2008) 3048–3055.
- [49] H. Yamaguchi, N.T. Woods, L.G. Piluso, H.H. Lee, J. Chen, K.N. Bhalla, A. Monteiro, X. Liu, M.C. Hung, H.G. Wang, p53 acetylation is crucial for its transcription-independent proapoptotic functions, *J. Biol. Chem.* 284 (2009) 11171–11183.
- [50] K. Han, C. Li, X. Zhang, L. Shang, DUXAP10 inhibition attenuates the proliferation and metastasis of hepatocellular carcinoma cells by regulation of the Wnt/beta-catenin and PI3K/Akt signaling pathways, *Biosci. Rep.* 39 (2019).
- [51] J.S. Liu, C.Y. Huo, H.H. Cao, C.L. Fan, J.Y. Hu, L.J. Deng, Z.B. Lu, H.Y. Yang, L.Z. Yu, Z.X. Mo, Z.L. Yu, Alopine induces apoptosis and G2/M cell cycle arrest in hepatocellular carcinoma cells through the PI3K/Akt signaling pathway, *Phytomedicine* 61 (2019) 152843.
- [52] X. Sun, M. Wang, F. Zhang, X. Kong, Inhibition of NET-1 suppresses proliferation and promotes apoptosis of hepatocellular carcinoma cells by activating the PI3K/AKT signaling pathway, *Exp. Ther. Med.* 17 (2019) 2334–2340.
- [53] X. Wang, K. Dong, Q. Jin, Y. Ma, S. Yin, S. Wang, Upregulation of lncRNA FER1L4 suppresses the proliferation and migration of the hepatocellular carcinoma via regulating PI3K/AKT signal pathway, *J. Cell. Biochem.* 120 (2019) 6781–6788.
- [54] P. Zhu, Z. Liu, J. Zhou, Y. Chen, Tanshinol inhibits the growth, migration and invasion of hepatocellular carcinoma cells via regulating the PI3K-AKT signaling pathway, *OncoTargets Ther.* 12 (2019) 87–99.
- [55] V. Nogueira, Y. Park, C.C. Chen, P.Z. Xu, M.L. Chen, I. Tonic, T. Untermyer, N. Hay, Akt determines replicative senescence and oxidative or oncogenic premature senescence and sensitizes cells to oxidative apoptosis, *Canc. Cell* 14 (2008) 458–470.
- [56] G. Augello, R. Puleio, M.R. Emma, A. Cusimano, G.R. Loria, J.A. McCubrey, G. Montalto, M. Cervello, A PTEN inhibitor displays preclinical activity against hepatocarcinoma cells, *Cell Cycle* 15 (2016) 573–583.
- [57] F. Buontempo, T. Ersahin, S. Missiroli, S. Senturk, D. Etro, M. Ozturk, S. Capitani, R. Cetin-Atalay, M.L. Neri, Inhibition of Akt signaling in hepatoma cells induces apoptotic cell death independent of Akt activation status, *Invest. N. Drugs* 29 (2011) 1303–1313.
- [58] D.M. Miller, S.D. Thomas, A. Islam, D. Muench, K. Sedoris, c-Myc and cancer metabolism, *Clin. Canc. Res.* 18 (2012) 5546–5553.
- [59] H.F. Zhang, C. Wu, A. Alshareef, N. Gupta, Q. Zhao, X.E. Xu, J.W. Jiao, E.M. Li, L.Y. Xu, R. Lai, The PI3K/AKT/c-MYC Axis promotes the acquisition of cancer stem-like features in esophageal squamous cell carcinoma, *Stem Cell.* 34 (2016) 2040–2051.
- [60] M.A. Chetram, C.V. Hinton, PTEN regulation of ERK1/2 signaling in cancer, *J. Recept. Signal Transduct.* Res. 32 (2012) 190–195.
- [61] J. Gu, M. Tamura, K.M. Yamada, Tumor suppressor PTEN inhibits integrin- and growth factor-mediated mitogen-activated protein (MAP) kinase signaling pathways, *J. Cell Biol.* 143 (1998) 1375–1383.
- [62] H. Chen, G. Zhu, Y. Li, R.N. Padia, Z. Dong, Z.K. Pan, K. Liu, S. Huang, Extracellular signal-regulated kinase signaling pathway regulates breast cancer cell migration by maintaining slug expression, *Can. Res.* 69 (2009) 9228–9235.
- [63] C.A. O'Brien, A. Pollett, S. Gallinger, J.E. Dick, A human colon cancer cell capable of initiating tumour growth in immunodeficient mice, *Nature* 445 (2007) 106–110.
- [64] X. Zhang, R. Hua, X. Wang, M. Huang, L. Gan, Z. Wu, J. Zhang, H. Wang, Y. Cheng, J. Li, W. Guo, Identification of stem-like cells and clinical significance of candidate stem cell markers in gastric cancer, *Oncotarget* 7 (2016) 9815–9831.
- [65] K. Nio, T. Yamashita, S. Kaneko, The evolving concept of liver cancer stem cells, *Mol. Canc.* 16 (2017) 4.
- [66] D.C. Kahraman, T. Kahraman, R. Cetin-Atalay, Targeting PI3K/Akt/mTOR pathway identifies differential expression and functional role of IL8 in liver cancer stem cell enrichment, *Mol. Canc. Therapeut.* 18 (2019) 2146–2157.
- [67] A. Rizzino, Concise review: the Sox2-Oct4 connection: critical players in a much larger interdependent network integrated at multiple levels, *Stem Cell.* 31 (2013) 1033–1039.
- [68] J. Shan, J. Shen, L. Liu, F. Xia, C. Xu, G. Duan, Y. Xu, Q. Ma, Z. Yang, Q. Zhang, L. Ma, J. Liu, S. Xu, X. Yan, P. Bie, Y. Cui, X.W. Bian, C. Qian, Nanog regulates self-renewal of cancer stem cells through the insulin-like growth factor pathway in human hepatocellular carcinoma, *Hepatology* 56 (2012) 1004–1014.
- [69] J.U. Marquardt, P.R. Galle, A. Teufel, Molecular diagnosis and therapy of hepatocellular carcinoma (HCC): an emerging field for advanced technologies, *J. Hepatol.* 56 (2012) 267–275.
- [70] N. Gawlik-Rzemieniewska, I. Bednarek, The role of NANOG transcriptional factor in the development of malignant phenotype of cancer cells, *Canc. Biol. Ther.* 17 (2016) 1–10.
- [71] H.L. Liu, H.T. Tang, H.L. Yang, T.T. Deng, Y.P. Xu, S.Q. Xu, L. Peng, Z. Wang, Q. Fang, X.Y. Kuang, Q.S. Li, Oct4 regulates the transition of cancer stem-like cells to tumor endothelial-like cells in human liver cancer, *Front. Cell Dev. Biol.* 8 (2020) 563316.
- [72] X.Q. Wang, W.M. Ongkeko, L. Chen, Z.F. Yang, P. Lu, K.K. Chen, J.P. Lopez, R.T. Poon, S.T. Fan, Octamer 4 (Oct4) mediates chemotherapeutic drug resistance in liver cancer cells through a potential Oct4-AKT-ATP-binding cassette G2 pathway, *Hepatology* 52 (2010) 528–539.

- [73] C.R. Jeter, M. Badeaux, G. Choy, D. Chandra, L. Patrawala, C. Liu, T. Calhoun-Davis, H. Zaehres, G.Q. Daley, D.G. Tang, Functional evidence that the self-renewal gene NANOG regulates human tumor development, *Stem Cell*. 27 (2009) 993–1005.
- [74] K. Zhang, M. Fowler, J. Glass, H. Yin, Activated 5'flanking region of NANOGP8 in a self-renewal environment is associated with increased sphere formation and tumor growth of prostate cancer cells, *Prostate* 74 (2014) 381–394.
- [75] H.F. Bahmad, K. Cheaito, R.M. Chalhoub, O. Hadadeh, A. Monzer, F. Ballout, A. El-Hajj, D. Mukherji, Y.N. Liu, G. Daoud, W. Abou-Kheir, Sphere-formation assay: three-dimensional in vitro culturing of prostate cancer stem/progenitor sphere-forming cells, *Front. Oncol.* 8 (2018) 347.
- [76] A.S. Rifaioğlu, E. Nalbat, V. Atalay, M.J. Martin, R. Cetin-Atalay, T. Dogan, DEEPScreen: high performance drug-target interaction prediction with convolutional neural networks using 2-D structural compound representations, *Chem. Sci.* 11 (2020) 2531–2557.